FLICKER SOURCE IDENTIFICATION AT A POINT OF COMMON COUPLING OF THE POWER SYSTEM

A THESIS SUBMITTED TO
THE GRADUATE SCHOOL OF NATURAL AND APPLIED SCIENCES
OF
MIDDLE EAST TECHNICAL UNIVERSITY

BY

ERİNÇ ALTINTAŞ

IN PARTIAL FULFILLMENT OF THE REQUIREMENTS
FOR
THE DEGREE OF MASTER OF SCIENCE
IN
ELECTRICAL AND ELECTRONICS ENGINEERING

MAY 2010

Approval of the thesis:

FLICKER SOURCE IDENTIFICATION AT A POINT OF COMMON COUPLING OF THE POWER SYSTEM

submitted by **Erinç Altıntaş** in partial fulfillment of the requirements for the degree of **Master of Science in Electrical and Electronics Engineering Department, Middle East Technical University** by,

Prof. Dr. Canan Özgen _____
Dean, Graduate School of **Natural and Applied Sciences**

Prof. Dr. İsmet Erkmen _____
Head of Department, **Electrical and Electronics Engineering**

Prof. Dr. Muammer Ermiş _____
Supervisor, **Electrical and Electronics Engineering Dept., METU**

Dr. Özgül Salor _____
Co-supervisor, **Power Electronics Group, TÜBİTAK UZAY**

Examining Committee Members:

Prof. Dr. A. Nezih Güven _____
Electrical and Electronics Engineering, METU

Prof. Dr. Muammer Ermiş _____
Electrical and Electronics Engineering, METU

Prof. Dr. Bülent Ertan _____
Electrical and Electronics Engineering, METU

Prof. Dr. Kemal Leblebicioğlu _____
Electrical and Electronics Engineering, METU

Dr. Osman Bülent Tör _____
Power Systems Group, TÜBİTAK UZAY

Date: 05 / 05 / 2010

I hereby declare that all information in this document has been obtained and presented in accordance with academic rules and ethical conduct. I also declare that, as required by these rules and conduct, I have fully cited and referenced all material and results that are not original to this work.

Name, Last Name: Erinç Altıntaş

Signature :

ABSTRACT

FLICKER SOURCE IDENTIFICATION AT A POINT OF COMMON COUPLING OF THE POWER SYSTEM

Altıntaş, Erinç
M.Sc., Department of Electrical and Electronics Engineering
Supervisor : Prof. Dr. Muammer Ermiş
Co-Supervisor : Dr. Özgül Salor

May 2010, 69 pages

Voltage fluctuations under 30 Hz in the electricity grid, leads to oscillations in the light intensity that can be perceived by human eye, which is called flicker. In this thesis, the sources of the flicker at a point of common coupling is investigated. When there are more than one flicker sources connected to a PCC, individual effects of each flicker source is determined by using a new method which depends on the reactive current components of the sources. This method is mainly based on the flickermeter design defined by the International Electrotechnical Commission (IEC), but uses the current variations in addition to the voltage variations to compute flicker. The proposed method is applied to several different types of loads supplied from a PCC and their flicker contributions on the busbar are investigated. Experiments are performed on field data obtained by the power quality analyzers (PQ^{+}) developed by the National Power Quality Project and the method has been found to provide accurate results for flicker contributions of various loads. The PQ^{+} analyzers with the proposed flicker contribution detection algorithm are called Flicker Contribution Meters (FC^{M}) and they will be installed at the points of the Turkish Electricity Transmission

Network when required.

Keywords: flicker contribution, flicker tracing, electric arc furnace (EAF), flickermeter, power quality (PQ), Flicker-Contribution-Meter (FC^M), point of common coupling (PCC).

ÖZ

GÜÇ SİSTEMLERİNDE ORTAK BAĞLANTI NOKTASINDA KIRPIŞMA KAYNAĞININ BELİRLENMESİ

Altıntaş, Erinç
Yüksek Lisans, Elektrik ve Elektronik Mühendisliği Bölümü
Tez Yöneticisi : Prof. Dr. Muammer Ermiş
Ortak Tez Yöneticisi : Dr. Özgül Salor

Mayıs 2010, 69 sayfa

Elektrik şebekesinde 30 Hz'in altıntaki gerilim salınımları, ışık şiddetinde kırpışma adı verilen ve insan gözüyle algılanabilen dalgalanmalara yol açar. Bu tezde ortak bir bağlantı noktasında kırpışmaya yol açan kaynaklar incelenmektedir. Ortak bağlantı noktasına bağlı bir ya da birden fazla kırpışma kaynağı olduğu durumda kırpışma kaynaklarının her birinin ortak bağlantı noktasında oluşturduğu etki, yüklerin reaktif akım bileşenlerini kullanan yeni bir yöntemle bulunmaktadır. Bu yöntem International Electrotechnical Commission (IEC) tarafından tanımlanan kırpışma ölçeri temel almakla birlikte kırpışmayı hesaplarken gerilime ek olarak akım değişimlerini de kullanmaktadır. Önerilen yöntem aynı ortak kuplaj noktasına bağlı çeşitli değişik yük tiplerinde kullanılmış ve bu yüklerin barada kırpışmaya olan katkıları araştırılmıştır. Güç Kalitesi Milli Projesi tarafından geliştirilen, Güç Kalitesi Çözümleyicileri (PQ^+) sistemleri kullanılarak alınan saha verileri üzerinde denemeler yapılmış ve önerilen yöntemin çeşitli yüklerin katkıları için doğru sonuçlar verdiği bulunmuştur. Önerilen kırpışma katkısı bulma yöntemiyle çalıştırılan güç kalitesi izleme sistemlerine Kırpışma Katkısı Ölçer adı verilmiştir (FC^M, Flicker Contribution Meter) ve bunlar Türkiye

Elektrik İletim Sisteminin çeşitli noktalarına ihtiyaç durumunda bağlanacaktır.

Anahtar Kelimeler: kırpışma katkısı, kırpışma kaynağıtakibi, elektrik ark ocağı, kırpışma ölçer, güç kalitesi , Kırpışma Katkısı- Ölçer (FC^M)

To my family

ACKNOWLEDGMENTS

I would like to express my deepest thanks and gratitude to my supervisor Prof. Dr. Muammer Ermiş for his guidance, advices, criticism and foresight throughout this research.

I would sincerely like to thank my co-supervisor Dr. Özgül Salor for her brilliant suggestions and comments, mental support and her confidence in me during my graduate studies. It would be impossible to finish this research work without her support and encouragement.

I would also like to express my thanks and gratitude to Prof. Dr. Işık Çadırcı for her elegant guidance and advices throughout this work.

I would specially like to thank to Alper Kalaycıoğlu and Dr. Turan Demirci for their support in software development. I would also like to thank the Power Quality Monitoring team of the National Power Quality Project for their technical support.

Special thanks to my colleagues B. Haliloğlu, Ö. Ünsar, S. Buhan, B. Boyrazoğlu, whom we worked together in the Mobile Power Quality Measurement team of National Power Quality Project for their support till the end of this research.

I would like to express my thanks to researchers and technicians of power electronics group of TUBITAK UZAY for their support.

I would like to thank Isdemir Iron and Steel factory for providing the data I have used in this thesis work.

I would like to thank iron and steel industry plants in the investigated region which let us collect data during their production process. They made collaboration with us during the measurements to provide us data for various operating conditions of the EAFs, which was not only time consuming but also costly for them.

This work has been fully supported by the Public Research Grant Committee (KAMAG) of TÜBİTAK within the scope of the National Power Quality Project (105G129). I would like to thank TÜBİTAK for making the ideas in this thesis a reality.

I also express my thanks to my friend H.E. Kale for his supports.

TABLE OF CONTENTS

LIST OF TABLES

TABLES

LIST OF FIGURES

FIGURES

CHAPTER 1

INTRODUCTION

Flicker is defined as the impression of unsteadiness of visual sensation induced by a light stimulus whose luminance or spectral distribution fluctuates with time [1]. This fluctuation of luminance is due to the voltage fluctuations on the terminals of the lamp. If the fluctuation of the voltage exceeds a certain amplitude versus frequency curve in Figure 1.1 which represents the lamp-eye-brain sensitivity, it causes an annoying effect on human eye. Surveys have been carried out on people by applying different voltage frequencies and magnitude changes and a curve is obtained such that more than 50 % of people perceives the light intensity change [2]. All the points on the curve in Fig 1.1 are defined to give a flicker severity equal to unity and the area above the curve is where the flicker becomes annoying for human beings.

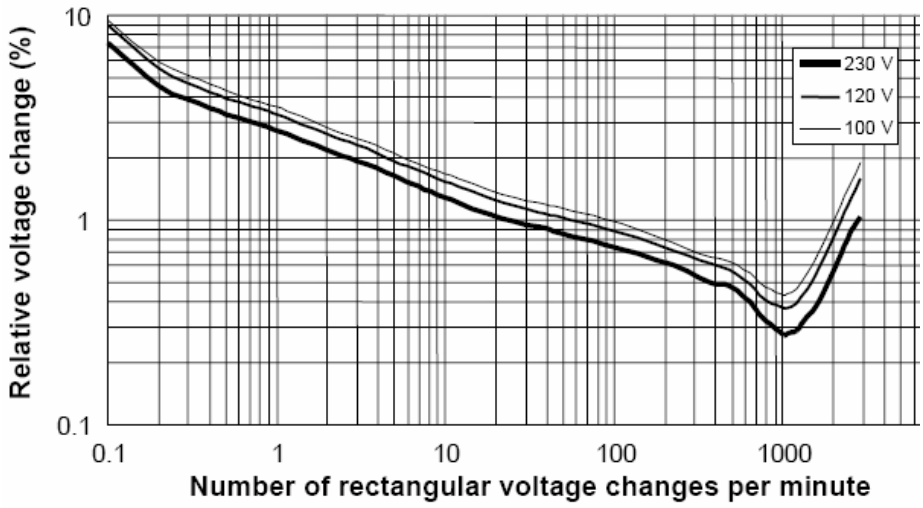

Figure 1.1: Flicker perception curve for square waveform modulated utility signal [3].

Flicker can be classified into two types which are cyclic and noncyclic. Cyclic flicker is due to the periodical changes of the voltage; on the other hand, noncyclic flicker is due to the stochastic changes [4]. The main flicker sources in the grid give rise to stochastic changes rather than periodical therefore the flicker observed is usually in noncyclic form.

In the cyclic case, the fluctuating signal that causes the flicker effect is an amplitude modulated waveform carried by the system frequency, which is 50 Hz. The square wave modulated signal in the IEC Standard [5] is shown in Figure 1.2. The percent voltage of a fluctuating signal is defined as

$$\begin{aligned} PercentVoltageModulation &= \frac{V_{max} - Vmin}{V_o} \times 100, \\ &= \frac{\Delta V}{V_o} \times 100. \end{aligned} \tag{1.1}$$

where,
V_{max} is maximum peak value of the modulated signal,
V_{min} is minimum peak value of the modulated signal,
V_0 is average value of the peak of the normal operating voltage.

The average value V_0 is defined on a 10-minute interval in most cases. The use of a normalization procedure by representing the voltage change in percentage, makes the flicker signal independent of the magnitude of the measured voltage [4].

The frequency range of the fluctuation is also as important as the percent voltage modulation, $\frac{\Delta V}{V}$. The frequency range which human eye can observe the flicker is between 0 and 30 Hz [4].

The amount of the flicker observed on a bus depends on several parameters.

- Size of the intermittent load,
- System impedance,
- Frequency of the voltage fluctuations [4].

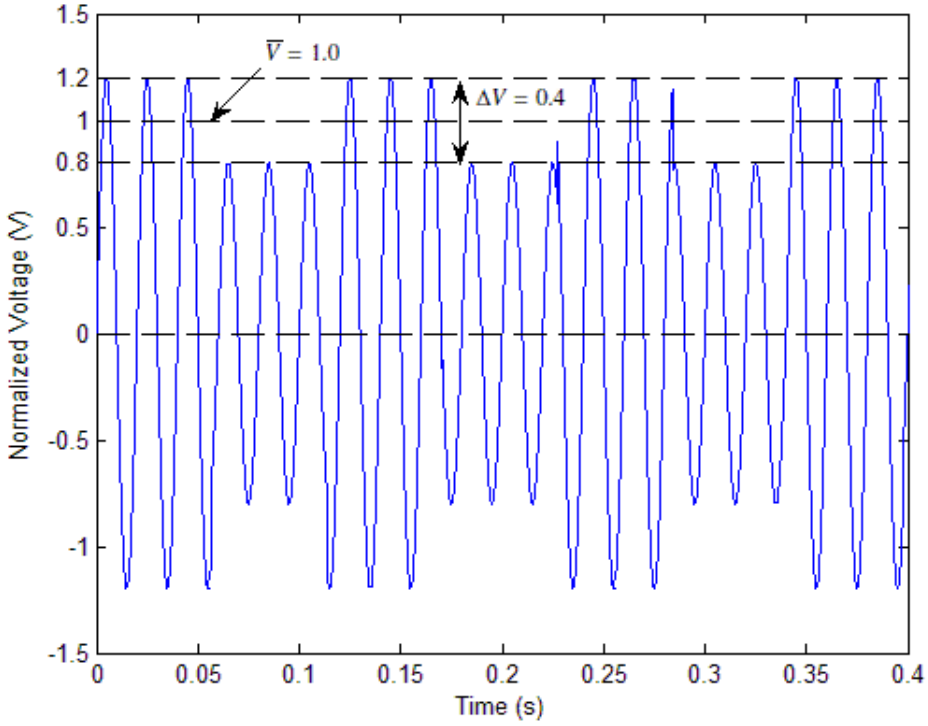

Figure 1.2: Square wave modulated signal with $\frac{\Delta V}{V_o} = \frac{40}{100}$ [5]

Flicker in the low voltage (LV) side is usually caused by highly fluctuating and intermittent loads supplied from the medium or high (MV or HV) voltage busbars, such as electric arc furnaces (EAF), ladle furnaces (LF), induction furnaces, and rolling mill plants. It is also caused by fluctuating loads on the LV side such as variable speed motor drives, air conditioning systems, X-ray equipment, copying machines, and etc. Flicker can affect the performance of the motors, reduce the life of electronic equipment, and can cause psychological problems such as stimulating the epilepsy.

The most common and severe load that causes flicker in an electrical network is an EAF. An EAF is a device used in metal industry where scrap metal is charged in a large furnace and electric arc is created to pass through the metal by using high power electrodes. By this way, melting of the scrap metal is achieved and prepared for further processes. This very stochastic process results in a highly fluctuating current and therefore a fluctuating voltage at the connected busbar. These voltage fluctuations also effect other customers connected to that busbar. Moreover, they can even be

transferred to low voltage busbars and affect the systems supplied from the lower voltage side.

In transmission networks, the power quality standards to be obeyed by the utilities apply on the common coupling points where many loads are supplied from. *The point of common coupling, (PCC) is the point where the utility connects to the end-user customer* [6]. It is also defined as *the point of a power supply network electrically nearest to a particular load, at which other loads are, or may be, connected* [7]. A typical transmission system is composed of interconnected transmission lines and loads at many different PCCs.

In order to calculate the severity of flicker, several techniques are proposed. In UK, Gauge-point voltage flicker meter was used which statistically analyzed the RMS fluctuations of voltage over a period of time. In Japan and eastern countries, equivalent 10 Hz voltage flicker (ΔV_{10}) method, which utilizes a spectrum analysis of the modulating signal and weights it according to a certain filter, is used. Later, the International Union for Electricity Applications (UIE) and International Electrotechnical Commission (IEC) has proposed an analog flickermeter that resembles the lamp-eye-brain response, and this flickermeter is being used for flicker analysis in most countries especially in Europe [5]. This is an analog device but thanks to the rapid advances in digital data acquisition, many digital flickermeters have been implemented so far.

The measurement of flicker at a PCC with any of these methods; however, does not provide information on the amount of flicker contributions of the loads and source side to the flicker measured at that PCC. Therefore, considerable amount of effort has been spent to determine the flicker contributions in the literature.

1.1 Literature Review

The topic of tracing flicker sources has gained more importance due to the increasing standards of the electric utilities. It is important to understand who is responsible of the flicker at the PCC by what percentage, not only to be able to take appropriate countermeasures, but also to be able to apply penalties defined by the correspond-

ing regulations fairly. Since flicker is a quantity defined on voltage, most of the researchers make use of the current variations to identify the flicker source. Some of the approaches concentrate on the direction of flicker, and try to clarify whether the main flicker source is a downstream source or an upstream source with respect to a PCC, as proposed in [8], [9], [10] and [11]. These methods are based on flicker power computation, V-I slope detection, and interharmonic power direction methods, respectively.

Some researchers concentrate on flicker power propagation inside the electricity transmission network [12], [13]. Flicker contributions from various flicker sources connected to a PCC have also been investigated [10], [11]. In [10], flicker contributions from various flicker sources are determined based on the flicker power direction analysis. The method proposed in [11] is based on the interharmonic power flow. These methods basically focus on the major flicker source determination, but not on the individual flicker contributions of various loads at the PCC.

However, determining how much each flicker source contributes to the flicker level at the PCC individually is more important than determining the main flicker source to be able to take appropriate and accurate countermeasures against deterioration of the power quality (PQ) at the PCC. Some researches concentrate on the issue of flicker contributions [14], [15], [2]. These researchers concentrated on the voltage drop caused from a customer that results in flicker. In [7], a similar method for evaluating the flicker resulting from wind power generators is proposed.

1.2 Problem Definition

Flicker at a PCC of the electricity transmission system is usually caused by more than one flicker sources. Determining the main sources of the flicker and finding out how much each source contributes to the flicker at the PCC is an important issue in order to apply appropriate flicker mitigation techniques to these flicker sources.

In this thesis, a new method based on reactive load current component variation is proposed to determine the flicker contribution of multiple loads supplied from a PCC to the flicker measured at the PCC. The method is based on the fact that, the variation

of the fundamental component of the voltage waveform in time causes the amplitude modulation effect, which results in flicker. It has been shown that this variation is mainly caused by the variation of the reactive power, and much less by the variation of the active power. The variation of the power (i.e. variation of the current drawn by the load) is primarily due to the highly fluctuating nature of some load types such as electric arc furnaces (EAFs). The proposed method decouples the flicker contribution of the interconnected system from the individual contributions of the loads connected to the measured PCC, by considering the individual current variations of the loads, and using the calculated short-circuit system impedance. This method is validated in the thesis by computations achieved on field data, which have been collected at a PCC, where multiple EAF plants are supplied from. The results show that the proposed method provides good estimates of the flicker.

The organization of the thesis is as follows: Chapter 2 describes the proposed method for finding the individual contributions of the loads connected to a common coupling point and verification of the method. In Chapter 3, application of the method on the field data is presented. The first part of this chapter presents results obtained by off line application of the method on the collected field data. In the second part, results of real time application of the proposed method is presented. The power quality monitors built to include the software of the real time application of the proposed flicker contribution method are called the Flicker Contribution Meters (FC^M). FC^M has the same hardware with the power quality analyzers developed in National Power Quality Project [16]. Chapter 4 describes the recommendations on the application of the flicker standard [5] based on the FC^M usage. Finally, Chapter 5 presents the conclusions.

CHAPTER 2

FLICKER CONTRIBUTION TRACING BASED ON INDIVIDUAL REACTIVE CURRENT COMPONENTS

In an interconnected electricity system, the flicker measured at a point of common coupling is not only caused by the consumer loads connected to that bus, but also by the transmission lines supplying power to the loads at that PCC. Buses in an interconnected electricity transmission system, have load feeders which consume power, transmission lines which supply power and feeders which may both consume and supply power. Unlike the radial systems, in the transmission systems the voltage waveform at a particular bus is formed by all of these effects.

2.1 Computation of the Source Side Effects and its Contribution on Flicker

In order to investigate the effects of source side at a PCC, a busbar in the transmission network is investigated in details. A detailed scheme of the investigated region is shown in Figure 2.1. In the investigated substation, ISKENDERUN-2, there are multiple scrap metal iron and steel furnace plants. One of these plants involves an AC arc furnace and one of them involves a DC arc furnace. These plants are both connected to the transmission bus at the 154 kV voltage level. Also there is one more scrap metal AC arc furnace plant which is connected to neighboring bus 3 km away from the investigated bus. D, A, and R+In in Figure 2.1, denote iron and steel plant based on DC EAF, iron and steel plant based on AC EAF, and rolling mill plus organized small industrial zone, respectively.

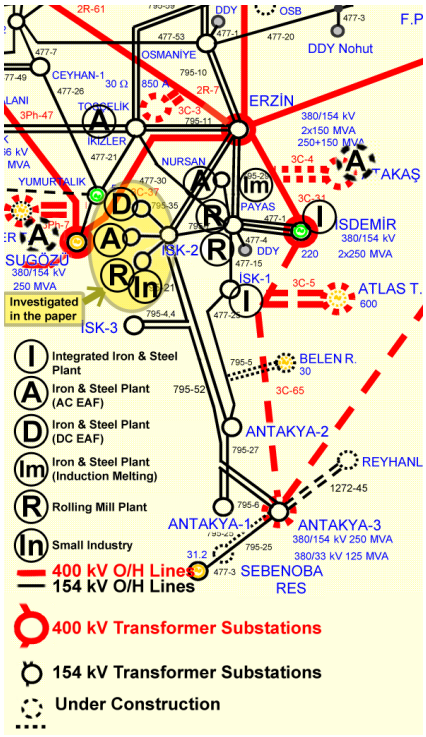

Figure 2.1: Connections of the investigated part of the Turkish transmission system.

In order to find out the characteristic of each feeder, all of the feeders connected to the busbar under investigation are measured. The power consumption of each feeder is calculated and depending on their load characteristics, they are listed as the load feeders which demand power all the time and the supply feeders. In Figure 2.2(a), eight feeders that are connected to the investigated busbar are measured synchronously. The total effect of the supply feeders in the interconnected system is now represented by an internal emf, E_s, and series source impedance $Z_s = R_s + jX_s$, based on the Thevenin's Network Theorem. A system with a hypothetical voltage source (E_s) and loads as shown in Figure 2.2(b) is constructed. In this model, Z_s represents the impedance seen by the loads supplied from the PCC. Therefore, Z_s is a representation of the rest of the interconnected system including the supply and all up-stream loads.

If the source voltage E_s remains constant during the measurement period, then the measured flicker level at the PCC would be only due to the variations in the loads. However, constant E_s is not expected in practical interconnected transmission systems, because the flicker effects of the other loads supplied from the other PCCs in

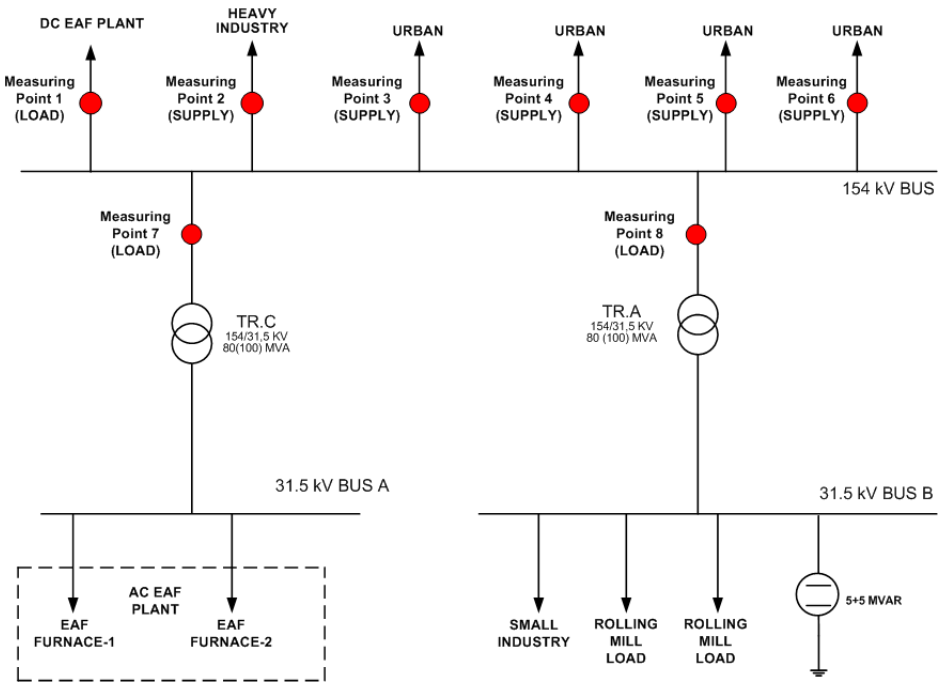

(a) Single-line diagram of the investigated substation and measurement points.

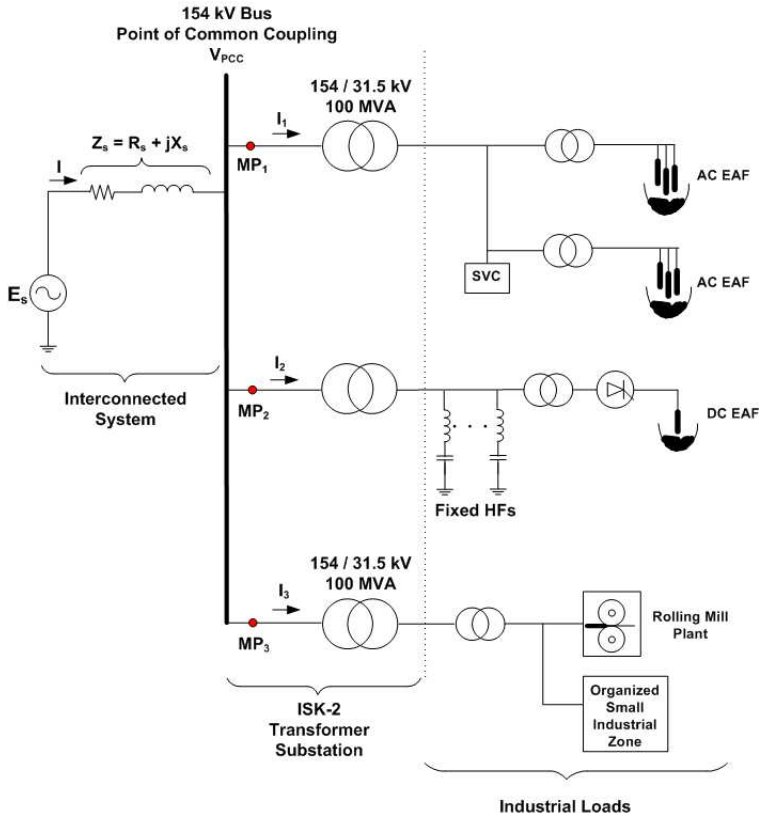

(b) Simplified single-line diagram of the investigated region of the electricity transmission system.

Figure 2.2: Single-line diagram of the investigated busbar.

the neighborhood will be partly transmitted to the bus under investigation and hence E_s will also be time varying. It is possible to experimentally determine whether E_s remains constant or not, by disconnecting all the loads from the PCC. It is obvious that this is impractical; therefore, fluctuations in E_s, which cause flicker at the PCC should be determined by field tests without interrupting the electricity service.

Time-domain value of the source side voltage ($e_s(t)$), in Figure 2.2(b), is obtained from

$$e_s(t) = R_s i(t) + L_s \frac{di(t)}{dt} + V_{PCC}(t) \tag{2.1}$$

where L_s is the inductance value obtained from X_s at the fundamental frequency, and R_s is the resistive component of the source impedance. Instantaneous values of voltages and currents, $V_{PCC}(t)$ and $i(t)$ are obtained from field measurements at a sampling rate of 25.6 kHz. Then, the amplitudes of the phasor, E_s, is obtained from the fundamental component (50 Hz) of amplitude values of one-cycle Discrete Fourier Transform (DFT) of $e_s(t)$. The variations of E_s in time obtained for the simplified diagram in Figure 2.2(b) which is deduced from the case in Figure 2.2(a) is shown in Figure 2.3. There are two different values of source side impedances in the graphs. The estimated Z_s is the system impedance estimated from the field measurements, and the calculated Z_s by PSS/E is the system impedance given by the utility by using the PSS/E load flow and short circuit simulations. The estimation of Z_s will be explained in details in Section 2.3. However it should be mentioned here that both Z_s values provide satisfactory results, while online estimation of Z_s give more accurate results for flicker computations.

In fact, this is an hypothetical solution, since $e_s(t)$ is not a directly measurable quantity. However, it is effective in showing the effects of the loads as well as that of the source side on the flicker level at the investigated bus. As observed in Figure 2.3(a), E_s is not constant and varies in time significantly. The voltage of the hypothetical source (E_s) is represented in pu values of the nominal busbar voltage in Figure 2.3.

When the voltage E_s is given as an input to the digital implementation of the flickermeter proposed by the IEC [5], the flickermeter's reading will contain the effect of the voltage variations coming from the source side (e_s) fluctuation of the fundamental voltage only. It should be noted that the input to the digital IEC flickermeter is the

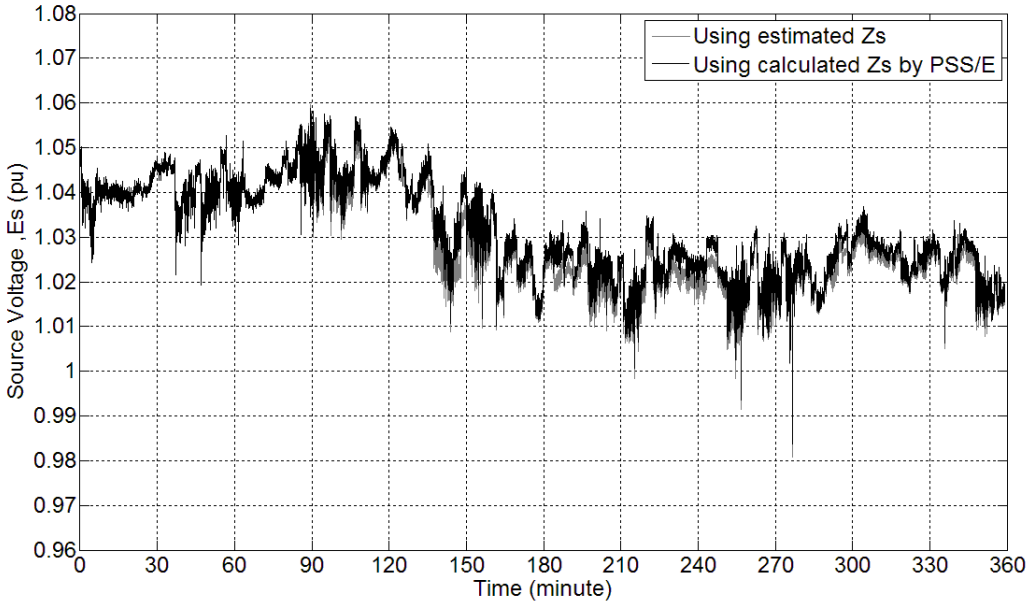

(a) E_s variations, (1-sec average)

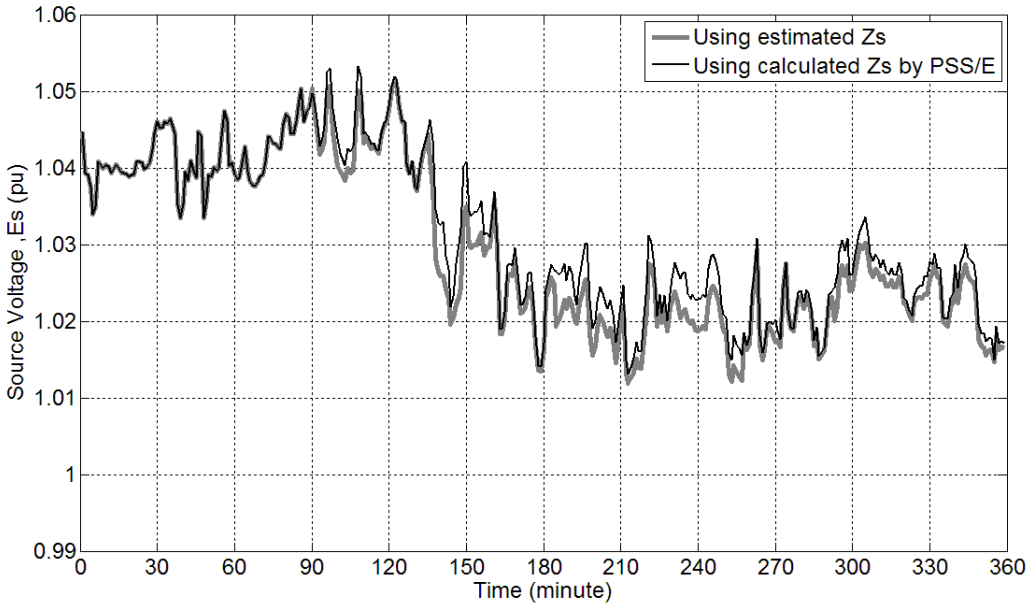

(b) E_s variations, (1-min average)

Figure 2.3: Variations of the hypothetical source voltage E_s.

peak value of the fundamental component of the source voltage. The output flicker P_{st} is given in Figure 2.4 with the IEC flickermeter results obtained from the voltage measured at the PCC for comparison purposes. The short term flicker severity presented here are evaluated in 1-min time intervals to observe the effects of rapidly-varying loads.

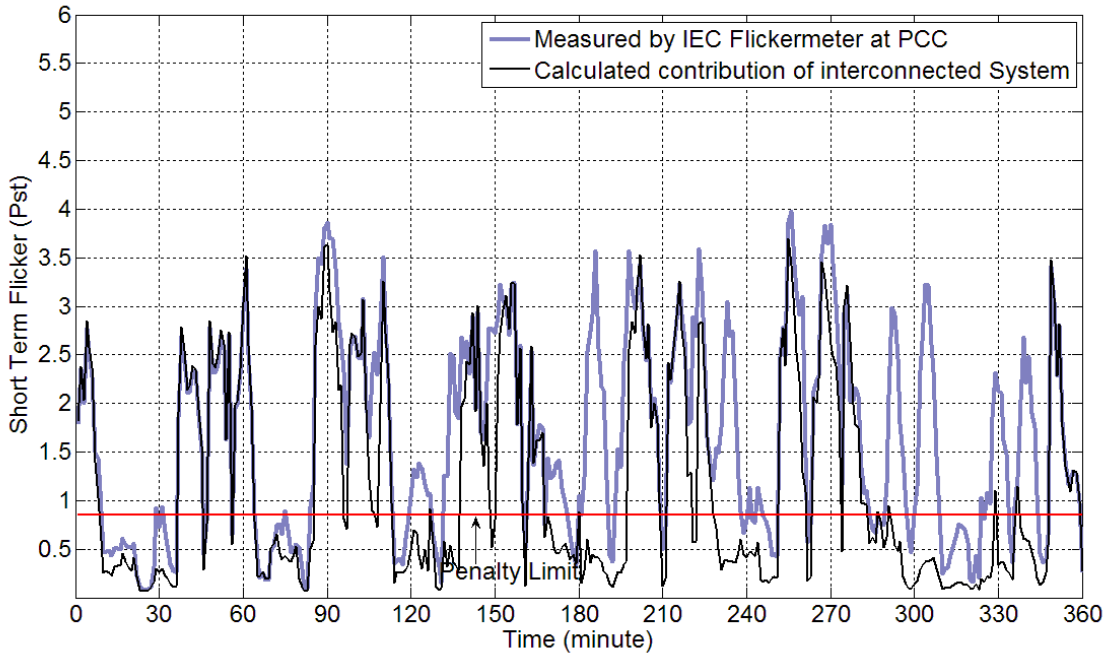

Figure 2.4: Flicker contribution of the source side(Interconnected System) compared with the IEC flickermeter measurement at the PCC

It is observed in Figure 2.4 that the flicker values differ significantly in particular periods. When the downstream loads are not demanding power, for example between 0 and 90 minutes, the load which has the biggest VA rating and which is the most probable to deteriorate the grid, is not operating and the flicker is mainly caused by the effects of neighboring upstream loads. The effects of the neighboring loads is transferred to the inspected bus via transmission lines (i.e the effect of the source voltage variation). In this 90 -min period, the two measured values do not differ much because the effect of the other loads in the busbar is not so dominant and nearly all the flicker at the busbar is caused by the source voltage variation. During the rest of the measurement period, the loads demand more power from the grid and the IEC flickermeter's reading, which is the total combined effect of the loads and the source

side, differs from the calculated contribution of the source side.

2.2 Computation of Individual Contributions of the Loads at the PCC

The voltage signal that causes flicker is the effect of an amplitude modulated signal as mentioned in Section 1.1. Since an electricity transmission system is not composed of ideal buses, any load connected to the grid is subjected to a system impedance. The change in the currents drawn by the loads gives rise to a voltage change in the bus which depends on the system impedance, magnitude and phase angle of the current with respect to the source voltage. A simple illustration of a load connected to a grid is shown Figure 2.5. Here, assume that E_s is an ideal voltage source and it remains constant. In the single load case as given in Figure 2.5, an increase in the current demand denoted by ΔI as given in Figure 2.5 will cause a voltage change ΔV at the PCC. This is due to the increased voltage drop on Z_s. Because, $V_{PCC} = E_s - Z_s \times I_{load}$ and hence $\Delta V_{PCC} = Z_s \times I_{load}$

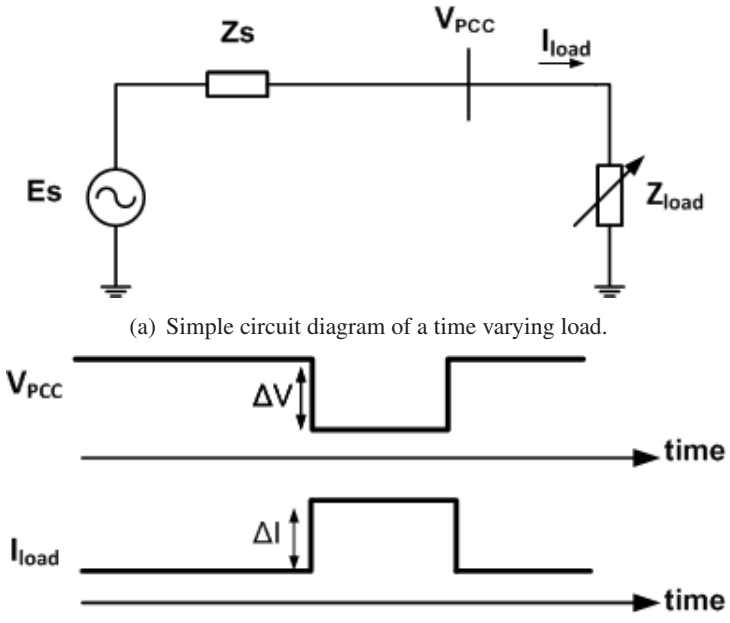

(a) Simple circuit diagram of a time varying load.

(b) Variations of PCC voltage and load current.

Figure 2.5: Simple circuit diagram of a time varying load.

In case of multiple loads, ΔI_{load} is the total effect of the demand changes of all loads. Therefore, one of the approaches to investigate the individual contribution of each

load is calculating the voltage drop in the system impedance, Z_s, by using only the individual load's current. In other words, computing this corresponds to the flicker level if and only if that load is connected to the grid. This approach, of course, uses the assumption that source voltage remains constant.

However, this not always the case. In an interconnected system, E_s cannot remain constant, but it is also time varying due to the effects of the upstream loads.

2.2.1 Mathematical Modeling

The phasor diagram of the relationship between E_s, I, Z_s, and V_{PCC} are given in Figure 2.6 and the associated vectorial equation is given as

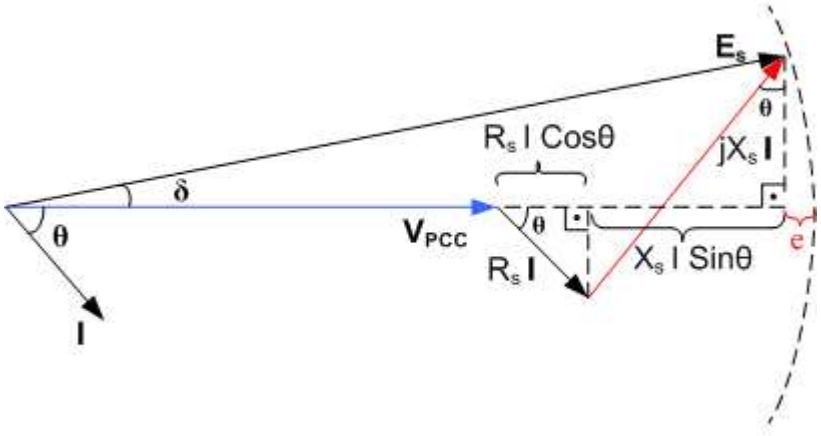

Figure 2.6: Illustration of the relationship between E_s, I and V_{PCC}.

$$E_s = Z_s \times I + V_{PCC}. \tag{2.2}$$

If one is going to design a flicker-contribution-meter based on (2.2), it requires vectorial computations to be carried out, which would complicate the process. However, the vectorial equation in 2.2 can be reduced to the algebraic equation in (2.3) based on the system specific assumptions for the system under investigation.

Equation 2.2 can be approximately rewritten as an algebraic equation as

$$E_s = V_{PCC} + R_s I \cos\theta + X_s I \sin\theta \tag{2.3}$$

under the below assumptions.

- δ is a small angle of the order of a few degrees. As an example, $\delta \approx 4$, when the loads demand 200 MW from the PCC.
- Since δ is too small, then $\sin\delta \approx \delta$ in radians;(For example $\sin\delta = 0.06976$, which is nearly $\delta = 0.06981$ and $\cos\delta = 1$.)
- R_s is smaller than X_s, that is X_s/R_s varies in the range from three to seven in a practical system.

The above properties imply that E_s and V_{PCC} are nearly in phase and hence the use of the algebraic equation in (2.3) is a good engineering approximation. Note that, $I\cos\theta$ and $I\sin\theta$ are the real and reactive components of the load current, respectively.

Furthermore, $R_s I\cos\theta$ is negligable in (2.3) in comparison with $X_s I\sin\theta$ for most of the operating conditions of EAF utilities, which results in,

$$E_s \approx V_{PCC} + X_s I \sin\theta. \tag{2.4}$$

Algebraic equation in (2.3) is called the *Complete Model*, and the equation in (2.4) is the *Simplified Model*. The method proposed in this thesis to trace the individual flicker contributions of loads, employs individual current measurements in addition to the voltage measurement at the PCC. Using the current measurements, potential drop on source impedance in case of the complete model ($R_s I\cos\theta + X_s I\sin\theta$) and the potential drop on X_s in the case of simplified model ($X_s I\sin\theta$), are calculated and then given as an input to a special flickermeter. This special flickermeter is called the *Flicker-Contribution-Meter* FC^M in the thesis. Since the proposed method does not employ E_s for flicker computation from individual loads, flicker contributions of loads are said to be decoupled from flicker contribution of the interconnected system at the PCC.

The block diagram of the proposed flicker-contribution-meter(FC^M) algorithm is given in Figure 2.7. PCC voltage and the the load current measured at MP_n in 2.2(b) are the inputs of the algorithm. θ and $|\ I\ |$ are computed with the help of the FFT block and they are used for ΔV_{PCC} computation as given in Figure 2.7. The IEC flickermeter is a part of the the algorithm with the input ΔV_{PCC}. Therefore, a brief introduction to the IEC flickermeter will be provided at this point to clarify the IEC flickermeter operation given in [5].

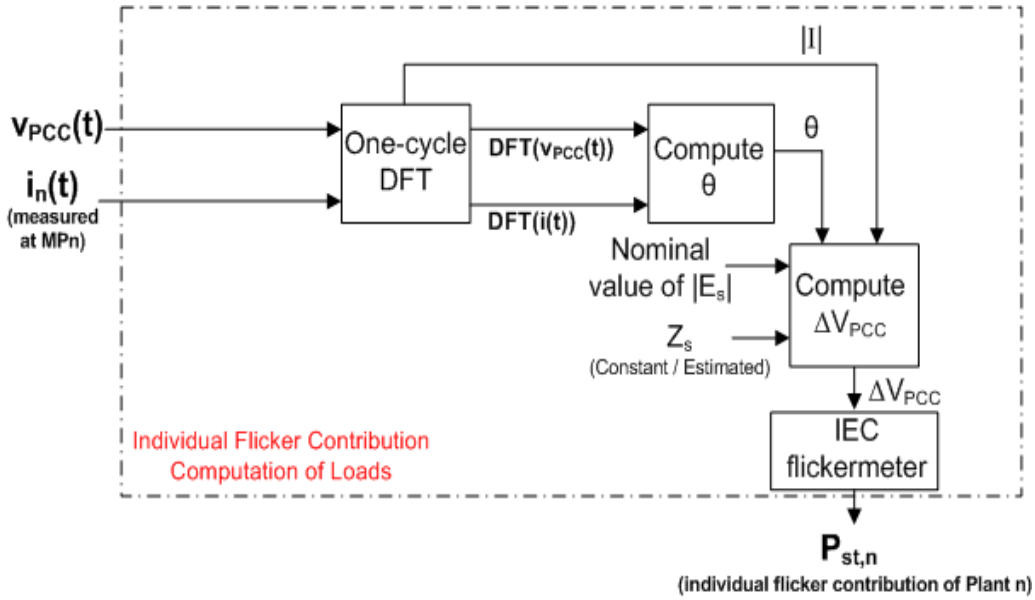

Figure 2.7: Method for tracing the individual flicker contributions of loads.

2.2.2 Usage of the IEC Flickermeter

The mathematical formula given in the Standard IEC $61000-4-15$, [5], for a square wave is given as

$$v(t) \quad = \quad V\sin(2\pi 50t)[1+\frac{\Delta V}{V}\frac{1}{2}\sin(2\pi f_{flicker}t)]. \tag{2.5}$$

It should be noted that ΔV given in the equation is the peak-to-peak value of the envelope, V is the rms value of the sine wave at 50 or 60 Hz, and $f_{flicker}$ is the flicker frequency. In normal operation conditions of a power system, the modulation in the

voltage is sinusoidal mostly instead of square wave hence the signum function in equation (2.5) is dropped.

By the product rule of the *sine* function the equation can be written as;

$$v(t) = V\sin(2\pi 50t) + \frac{\Delta V}{4}[\cos(2\pi(50 - f_{flicker})t) - \cos(2\pi(50 + f_{flicker}))t]. \quad (2.6)$$

It is observed that the signal is composed of fundamental components and the inter-harmonics at the frequencies $50 \pm f_{flicker}$. This signal is demodulated by a squaring block and a low-pass filter in the IEC flickermeter. The operating principles of the IEC flickermeter are explained in Appendix A in detail.

Since the envelope of the voltage waveform at the PCC for the case when only the corresponding load were supplied, is the ΔV_{PCC} as given in Figure 2.7, the demodulation block of the IEC flickermeter is not used in the proposed algorithm. ΔV_{PCC} is supplied to Block 1 given in Figure A.1 in Appendix A and P_{st} is obtained at the output of Block 5.

There are two outputs of the FC^M. One is the actual flicker value at the inspected bus, the other is the contribution of the specific feeder to the flicker level by using the system impedance given by the utility.

2.3 Estimation of the Source Side (Upstream) Impedance

The actual value of the source side impedance can only be calculated by the utility from actual network data based on all system parameters, load configurations and load data. It is usually a very hard task to predict the load types and the configuration for a particular time of the network even for the system operator. Different kinds of loads affect the system impedance in different manners. For example, a dynamic load like an induction motor would contribute to the short circuit current in case of a fault at that bus while a resistive load would not.

The application of the proposed flicker contribution detection method requires the source side impedance, Z_s, seen from the load side at the PCC to be known. There are two methods to estimate Z_s. It can be either taken as the constant value provided

by the utility, or it can be estimated using a source impedance estimation method.

2.3.1 Z_s Estimation from Field Data

Estimation of the $Z_s(= R_s + jX_s)$ values based on the measured data provides more realistic values, since the impedance is computed deploying the instantaneous values of the voltage and current measurements. Changes due to different load conditions of the interconnected system are followed by the Z_s estimation method. The method proposed in [17] is used for Z_s estimation.

For Z_s estimation based on field data, time-synchronous voltage and current measurements (with time-synchronization accuracy less than 100 nsec.) are carried out by the permanent PQ^+ Analyzers developed through the National Power Quality Project of Turkey . The time-synchronization is achieved by the GPS module integrated into the PQ^+ Analyzers. The sampling rate of each voltage and current waveform is 25.6 kHz, and it is down-sampled to 3.2 kHz for the analysis in this section. The method utilizes the natural variations in the voltage and current values. Since the load under investigation is highly fluctuating, the correlation between the voltage change and current change gives an estimate for the impedance seen from the load side.

The total load current, $i(t)$, is obtained by summing up the currents. $i(t)$ and $v(t)$, which is the voltage measured at the PCC, is used to estimate Z_s based on the method given in [17]. Fundamental components of $i(t)$ and $v(t)$, denoted by $\mathbf{I}$ and $\mathbf{V}$ in phasor domain respectively, are computed by deploying one-cycle DFTs of the waveforms. According to [17], Z_s is given as

$$\Delta V_{PCC} = -Z_s \Delta\, I_{load} \tag{2.7}$$

where $\Delta\ V_{PCC}$ is the change in phasor V_{PCC} from one cycle to the one after next, while ΔI_{load} is the change in phasor I_{load} from one cycle to the one after next. For this method to be valid for Z_s computation, variation of the voltage ΔV_{PCC} should be a consequence of the variation in current ΔI_{load} (i.e a downstream event occurs).

For the simple model shown in Figure 2.5, $\Delta V_{PCC} = V_{i+2} - V_i$ is introduced where V_i

and V_{i+2} are the two consecutive phasor values of $V_{PCC}$and the subscript i represents the cycle counter.

According to [17], for this to be satisfied the below equations should hold:

$$|\Delta I| \geq 100A, \tag{2.8}$$

$$\frac{|\Delta V|}{|\mathbf{V}|} \geq 0.01 \tag{2.9}$$

If the current drawn by the load is more than 100 Amperes and if it gives rise to a voltage drop of 1% of the voltage measured, the impedance is calculated by the equation (2.7). Another advantage of using these criteria is that it is possible to eliminate the erroneous impedance calculation due to the low accuracy of voltage and current transformers. The voltage and current measurements are taken from the secondary terminals of protection type voltage and current transformers since usually there is no metering on the high voltage level (154 kV). Therefore the accuracy class of current transformers are class 10P (i.e ±%3 at rated current) which is a quite high ratio.

The magnitude, Z_{mag} and the angle Z_{phase} of the impedance Z_s ar computed and hence system the system resistance, R_s, and the system reactance, X_s are determined as

$$R_s = Z_{mag}\cos(Z_{phase}), \tag{2.10}$$

$$X_s = Z_{mag}\sin(Z_{phase}). \tag{2.11}$$

Z_s values for cycles satisfying the given criteria are computed and the computed Z_s values are collected for periods of 10 min, which correspond to 30,000 values of Z_s for each 10-min window of the data. However, since the criteria is not always satisfied, especially when the EAFs are in the refining and charging phases where the current is not significantly fluctuating, this number is usually much less than 30,000. If in a 10-min period, the number of ΔV and ΔI pairs satisfying the criterion is less than 1,000, then Z_s is not estimated for that 10-min period, but the Z_s value of the previous 10-min period is used instead.

The estimated impedance values are then subjected to a statistical evaluation according to [17]. The histogram of the impedance magnitudes and angles are obtained. A bin step of 0.01 is used for magnitude and 0.1π is used for the angle classifications. These histograms show where system impedance is more likely to be. The median of the values in the histogram plots are found to be the ultimate estimated phase and magnitude of that 10-min period. The histogram obtained from one of the 10-min periods of the field data is shown in Figure 2.8(b) to provide an insight on the source impedance distribution.

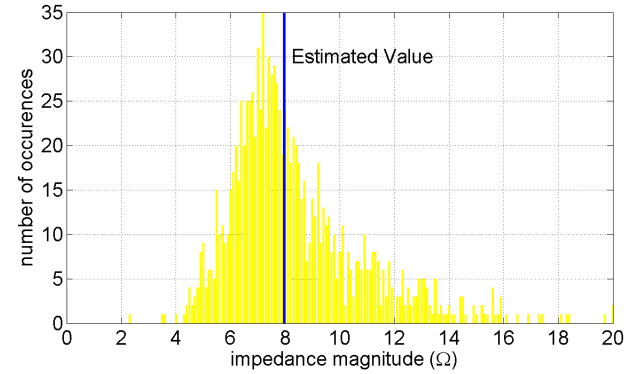

(a) Magnitude Histogram.

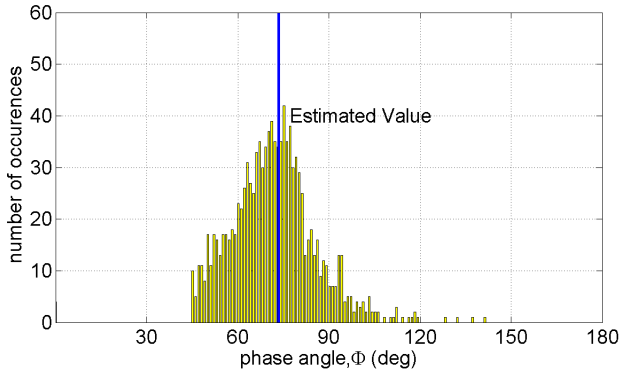

(b) Angle Histogram.

Figure 2.8: Statistical source impedance estimation.

This computation is achieved for every 10-min interval with a sliding window of 1-min which is located in the middle of the 10-min period in time axis. Hence a new system impedance is estimated for each minute. In Figure 2.9, these estimated values are shown together with the system impedance values provided by the utility for a bus investigated in region 13 of the Turkish Transmission System. It is worth to note that

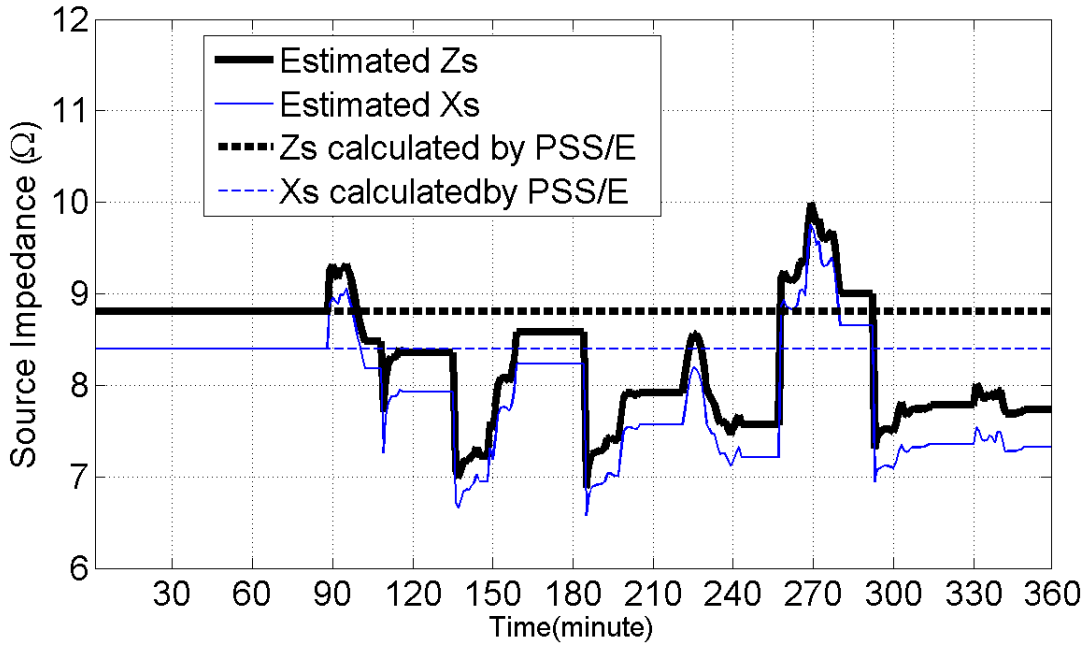

Figure 2.9: Comparison of the magnitudes of the source side impedances and reactances obtained by estimation and computed by the utility using PSS/E

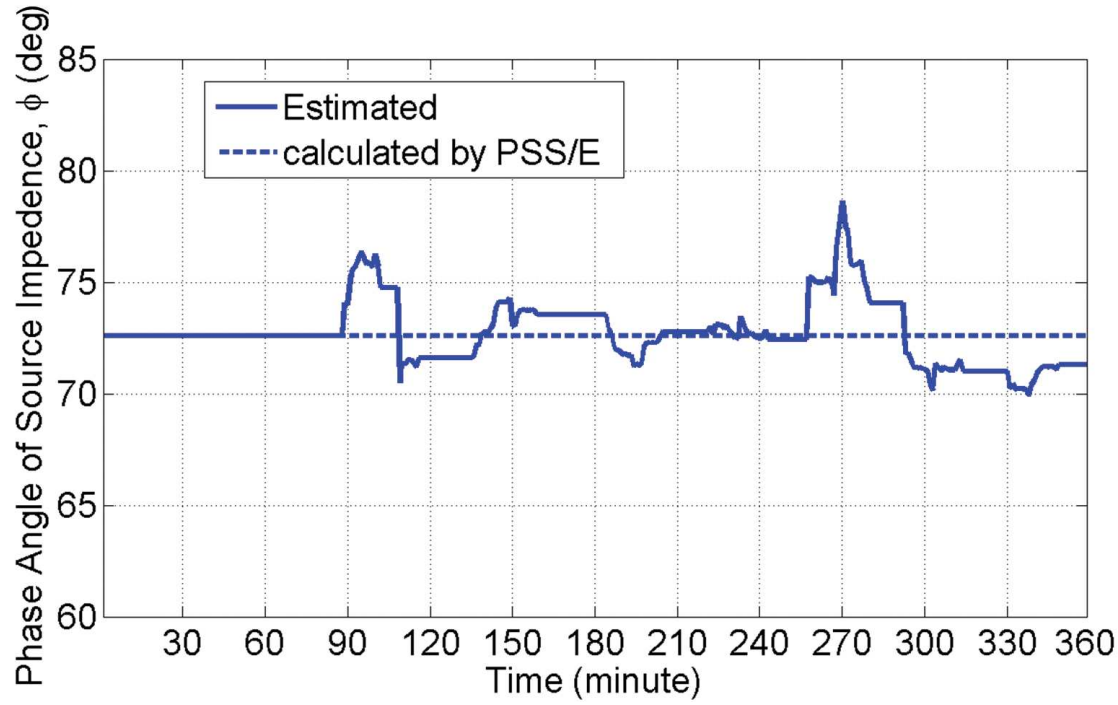

Figure 2.10: Comparison of the angles of the source side impedances obtained by estimation and computed by the utility using PSS/E

from 0 to 90 min period in Figure 2.9, the voltage and current changes do not satisfy the above given criteria and no Z_s estimation is achieved. Since any previous Z_s does not exist at the beginning of the computations, Z_s values obtained from PSS/E (Power System Simulator for Engineering) simulations are used as the initial value of Z_s.

2.3.2 Z_s Estimation by the Utility

Minimum and maximum values of Z_s for specific location of the transmission system for both summer and winter periods are computed by the utility based on PSS/E simulations run on field data obtained from the entire interconnected system. Z_s values are calculated from the short circuit currents seen from the load side at a certain PCC of the utility. The short circuit current values provided by the system operator, for the ISK-2 PCC in Figure 2.1 are given in Table 2.1.

Table 2.1: The short circuit current values provided by the system operator for ISKENDERUN-2 154 kV Bus

2008 Minimum Load	10.0633 kA
2008 Summer Peak Load	10.0633 kA
2008 Winter Peak Load	12,2336 kA

However, the use of a constant value for Z_s, determined by running PSS/E program for the specific measurement day, gives correct results only if the interconnected system is widely monitored by a SCADA (Supervisory Control and Data Acquisition) system accurately. For the Z_s estimation to be precise, the PSS/E simulation should be repeated frequently so that demand changes are represented clearly. Therefore, flicker contributions of the loads determined by using the constant value of the Z_s mentioned above are to be compared with the FC^M measurements based on time-varying Z_s. For the PCC given in Figure 2.2(a), we have compared the Z_s values provided by the utility with the Z_s computed from field data, for a measurement period of 6 hours. Results are given in Figures 2.9 and 2.10. FC^M measurements with constant Z_s, are almost the same with those as time varying Z_s. It can, therefore, be concluded that the FC^M can be programmed with the simplified model employing constant Z_s value in order to make the FC^M measurements practical with sufficient accuracy. If precise measurements are required, Z_s computation from field data will be necessary.

2.4 Verification of the Method on Synthetic Data and Field Data

Verification of the proposed method is first achieved by comparing the short term flicker value, P_{st}, measured at PCC by the IEC flickermeter, with the P_{st} values computed by the proposed method. Then, the flicker demodulation technique is verified on synthetic data.

2.4.1 Verification of the Flicker Computation at the PCC

The block diagram of the verification process is illustrated in Figure 2.11. One-cycle DFTs with non-overlapping windows are used to compute the magnitudes and the phases of the fundamental components of the total load current, $i(t)$, and the voltage at PCC, $V_{PCC}(t)$. $e(t)$ is computed based on Equation (2.1) and from the DFT of $e(t)$, amplitude of the fundamental component is extracted as $|E_s|$. The variation of $|E_s|$ contributes from the source side to the flicker at PCC. The total variation of the voltage at the PCC, ΔV_{PCC}, is determined from the complete model in Equation 2.3. Then ΔV_{PCC} is given as input to the IEC flickermeter to compute the P_{st} at the PCC.

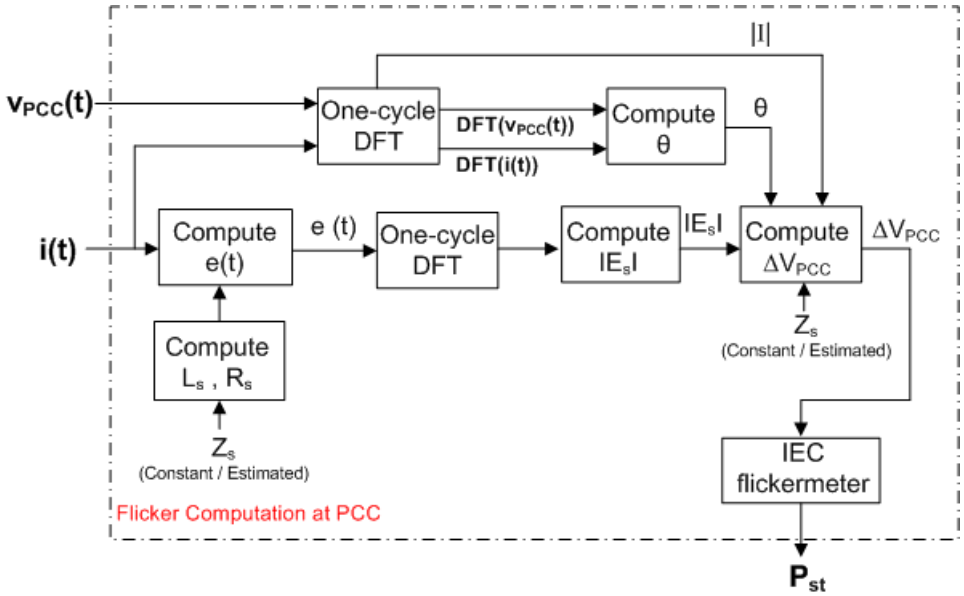

Figure 2.11: Block Diagram of the procedure for verifying the flicker at the PCC.

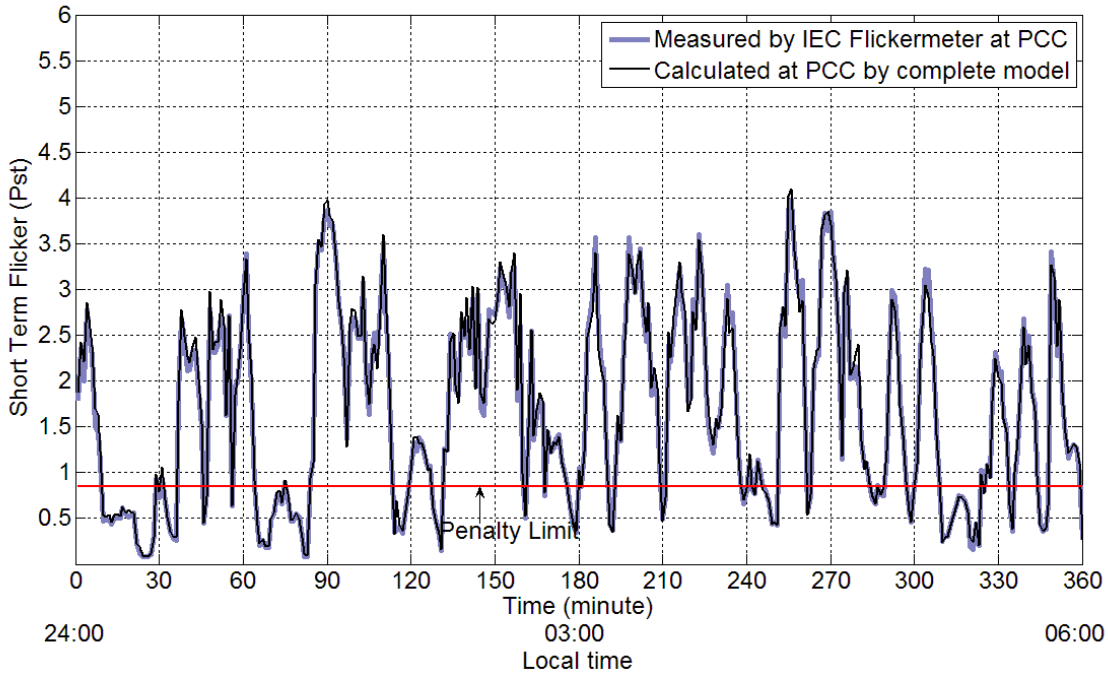

Figure 2.12: Flicker Computed at PCC, both by the proposed method and the IEC flickermeter.

In order to verify the results of the proposed flicker computation method, the measured 1-min P_{st} values at the PCC by the IEC flickermeter for the whole six-hour measurement period for the case given in Figure 2.2(b) are compared with the values obtained by the method in Figure 2.11. As illustrated in Figure 2.12, the flicker levels at the PCC calculated from the complete model match closely with the IEC flickermeter measurements.

Since it is not possible to eliminate the effect of source side in a real system, a simulation of 30 minutes in EMTDC/PSCAD environment is achieved for an arc furnace load. Such a simulation allows us to keep the source voltage, $|E_s|$, constant. The simulation environment is given in Figure 2.13.

The current of the EAF plant obtained from field measurements for a period of 30 min is used as a controlled current source in the simulation. A source with constant voltage magnitude is used as given in Figure 2.13 . The same frequency and phase with the measured PCC voltage is provided to the source voltage assuming that the

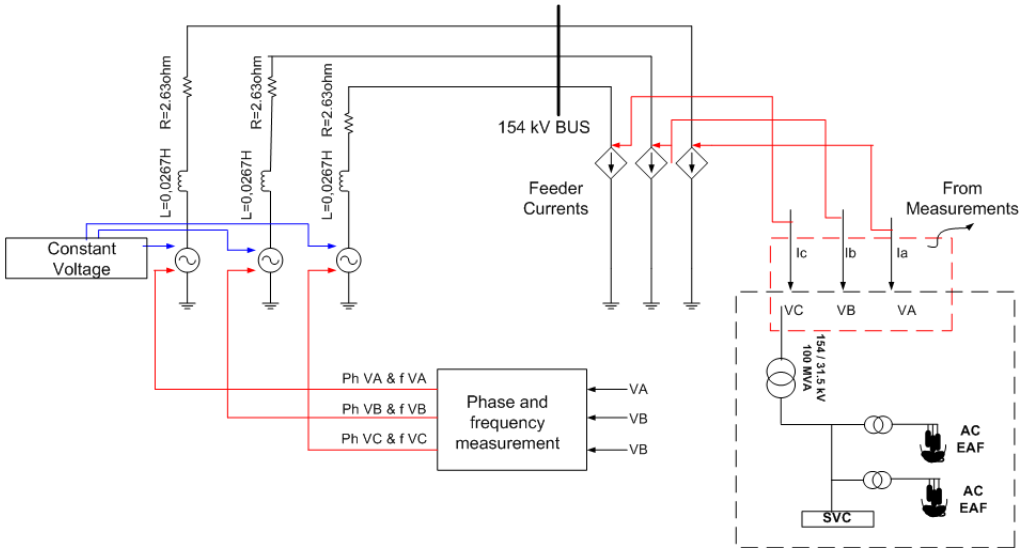

Figure 2.13: Simulation environment to compare the flicker computed by the proposed method and the IEC flickermeter.

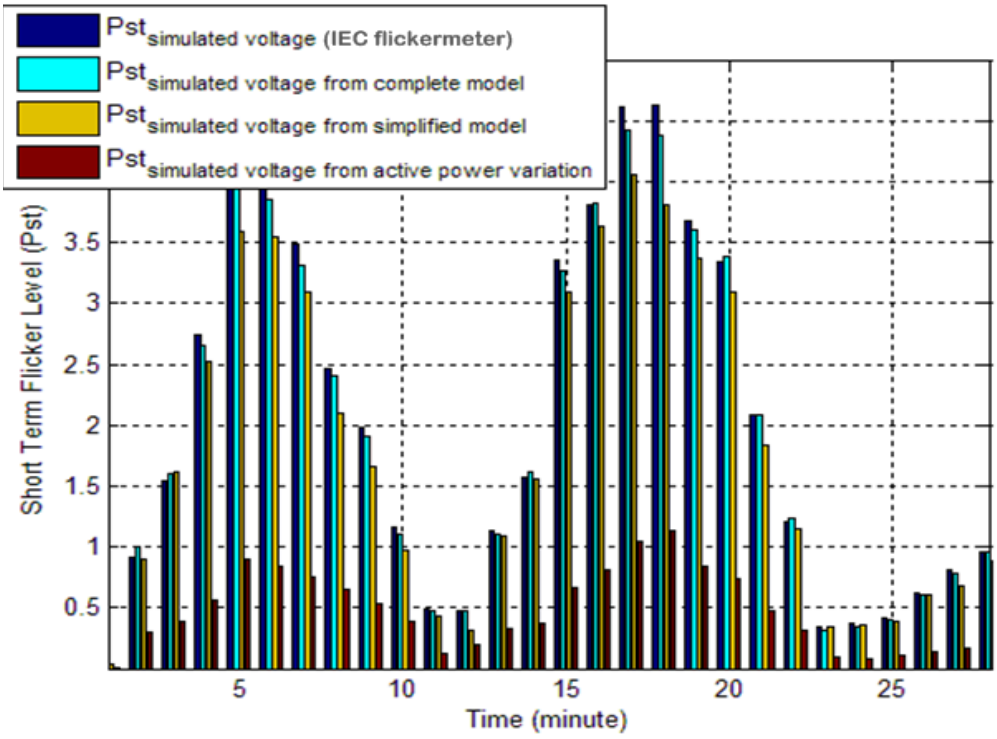

Figure 2.14: Comparison of the IEC flickermeter & various cases of the proposed method for 30 min Pst measurements obtained at the PCC in Figure 2.13.

angle between V_{PCC} and E_s is much smaller than the angle between I_{load} and V_{PCC}. This procedure is to make sure that the angle between the load current and the voltage at the PCC is correct.

The impedance of the grid is assigned to be the same as given by the utility company. Since the impedance is very well known and the source side voltage magnitude is not fluctuating, the resultant flicker measured on the simulated value of voltage evaluated provides the value of the flicker only due to the EAF plant and hence the source side effects is eliminated. The flicker values at the PCC voltage for various cases of the proposed method and measured by the IEC flickermeter are compared in Figure 2.14. It is observed that the complete model estimates the flicker with high accuracy and the simplified model is also quite accurate. The affect of the active power variation to the flicker is also given in the Figure and it is observed that active power variation has low affect on the flicker.

2.4.2 Verification of the DFT-Based Demodulation Technique

To verify the usage of one-cycle (20 msec for 50 Hz signal) DFT method to find the modulation affect of the flicker frequency, the test procedure explained by the block diagram given in Figure 2.15 is used. An example modulation of the sine wave is represented in Figure 2.16. One-cycle DFTs are used to determine the amplitude

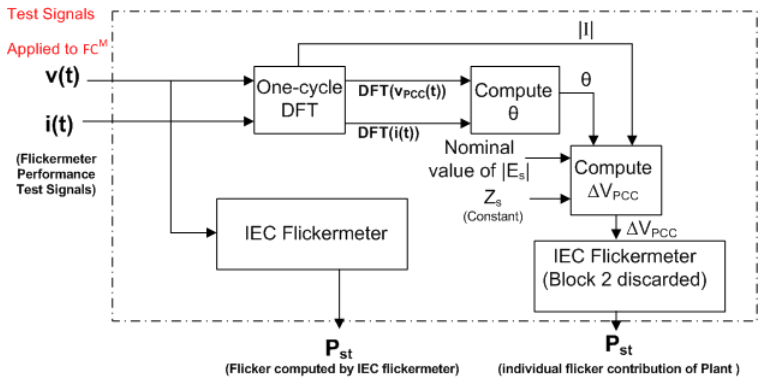

Figure 2.15: Block diagram of the test procedure for the DFT-based demodulation algorithm.

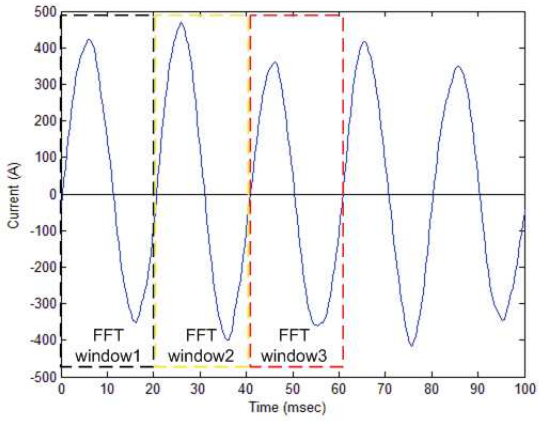

(a) The FFT window.

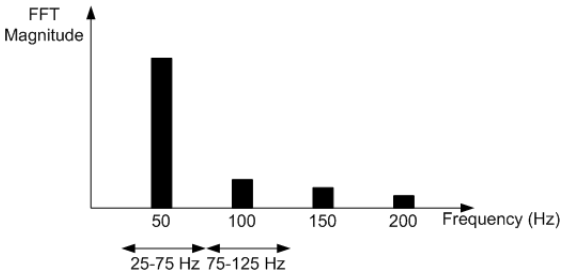

(b) Resolution of the FFT for one of the windows.

Figure 2.16: One-cycle FFT windows.

changes in the fundamental component of the signal. One-cycle DFT corresponds to a DFT output of 50 Hz resolution. The variation of the fundamental component from one cycle to the next gives the modulation effect of the flicker component as can be deduced from (2.16) & (2.17).

For this verification step, V_{test} signal is directly applied to the IEC flickermeter and the FC^M as given in Figure 2.15 and the results are compared. V_{test} are the test signals to obtain $P_{st} = 1$ (Table 2.2(a)) given in the IEC standard [5]. Tests are also repeated for $P_{st} = 2$ & $P_{st} = 3$ (Table 2.2(b) and (c))and the results are given in Table 2.2. In all these cases the flicker output should be in the ±5% accuracy according to [5].

The FC^M device is tested for P_{st} measurement accuracy with the performance signals given in the IEC Flickermeter Standard [5]. The IEC flickermeter and FC^M readings are compared. It is expected that both outputs should give $P_{st} = 1 \pm 0.05$ for the given test signals in (a). For (b) and (c), P_{st} is expected to be 2 ± 0.1 and 3 ± 0.15,

respectively. It is observed that the demodulation method using DFT provides quite accurate results, except for the 33.33 Hz flicker frequency. This is due to the fact that computing the amplitude every cycle corresponds to an analysis of 50 Hz sampling rate for the fundamental amplitude and therefore, for flicker frequencies (which is also the amplitude modulation frequency) above 25 Hz, the method does not give accurate results. However, it should be noted that flicker frequencies larger than 25 Hz are not usually observed in the practical systems [4]. Therefore, results on field data as given in Figure 2.17, shows that DFT demodulation provides accurate P_{st}s and instantaneous flicker levels, IFLs (output of Block 4 in Figure A.1).

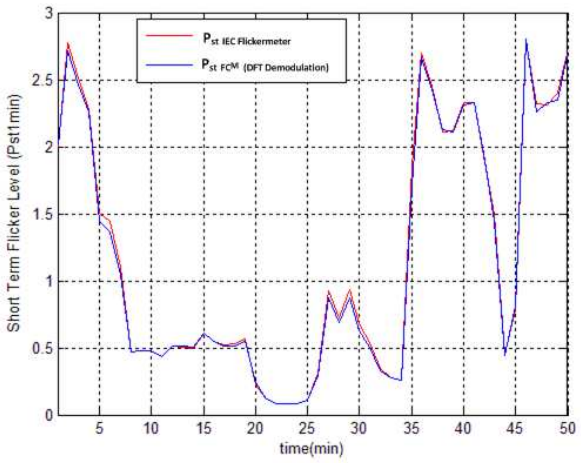

(a) Flicker variations

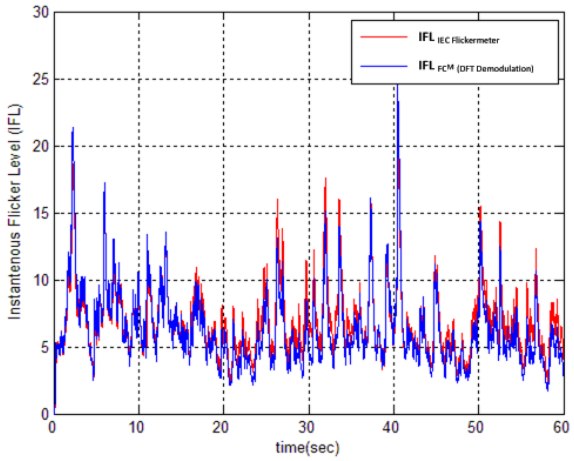

(b) IFL variations

Figure 2.17: Flicker values calculated with two different demodulation techniques

Table 2.2: Comparison of the P_{st} Measured by IEC Flickermeter and the FC^M Using the Test Signals Given in IEC-61000-4-15 [5]

(a)

$\Delta V/V(\%)$	Change per minute $\backslash frequency(Hz)$	The expected value $P_{st} = 1 \pm 0.05$	Output of IEC Flickermeter	Output of FC^M
2.724	1 \0.0083	1 ± 0.05	0.97232666	1.016363531
2.211	2 \0.0166	1 ± 0.05	0,99268190	1,037805289
1.459	7 \0.0583	1 ± 0.05	1,00137559	1,041466466
0.906	39 \0.3250	1 ± 0.05	1,00907893	1,049860558
0.725	110 \0.9166	1 ± 0.05	0,98907067	1,028997523
0.402	1620 \13.5	1 ± 0.05	0,96089243	0,924514316
2.4	4000 \33.333	1 ± 0.05	1,00264648	1,494800218

(b)

$\Delta V/V(\%)$	Change per minute $\backslash frequency(Hz)$	The expected value $P_{st} = 2 \pm 0.1$	Output of IEC Flickermeter	Output of FC^M
2x2.724	1 \0.0083	2 ± 0.1	1,943548912	2,032727972
2x2.211	2 \0.0166	2 ± 0.1	1,984466138	2,075611328
2x1.459	7 \0.0583	2 ± 0.1	2,002393259	2,0829477
2x0.906	39 \0.3250	2 ± 0.1	2,017937349	2,099721519
2x0.725	110 \0.9166	2 ± 0.1	1,977991707	2,057987424
2x0.402	1620 \13.5	2 ± 0.1	1,921698943	1,849034083
2x2.4	4000 \33.333	2 ± 0.1	2,005187257	2,979654822

(c)

$\Delta V/V(\%)$	Change per minute $\backslash frequency(Hz)$	The expected value $P_{st} = 3 \pm 0.15$	Output of IEC Flickermeter	Output of FC^M
3x2.724	1 \0.0083	3 ± 0.15	2,912613389	3,049093316
3x2.211	2 \0.0166	3 ± 0.15	2,974717993	3,113418125
3x1.459	7 \0.0583	3 ± 0.15	3,002794325	3,12439545
3x0.906	39 \0.3250	3 ± 0.15	3,026595665	3,149582859
3x0.725	110 \0.9166	3 ± 0.15	2,966755114	3,086983872
3x0.402	1620 \13.5	3 ± 0.15	2,882488833	2,773558976
3x2.4	4000 \33.333	3 ± 0.15	3,006892134	4,485726515

2.5 Summary

This section presents the basics on which the proposed flicker-contribution-meter computations are based on. The flicker contributions of the loads supplied from a PCC and the contribution of the source-side (upstream loads and generators) can be computed with the help of the proposed method. The method depends on the fact that, the variation of the reactive component of the current drawn by the loads is the dominant reason of the variation of the voltage at the PCC , which creates flicker. If there is no variation in the reactive currents of the loads, then the flicker measured at the PCC is due to the supply side. Therefore, the computation of the voltage drop on the source side impedance, Z_s caused by the individual current of each load , decouples the flicker effect coming from the source side, and gives individual flicker contribution of the load. In fact, the flicker-contribution-meter FC^M developed throughout this thesis work, computes the flicker to be measured at the PCC if it were the only flicker-causing load supplied from the PCC, and there were no flicker effect coming from the source-side.

The method requires the source side impedance seen from the PCC to be known. Two methods were proposed for Z_s estimation. Either the Z_s estimated by the utility is used, or Z_s is computed on-line from the collected voltage and current data. It has been shown that both estimations provide satisfactory results for flicker contribution computations, however, for most accurate results online Z_s estimation should be preferred. The source side impedance is estimated for every 1-min time period, while ΔV in Equations 2.3 and 2.4 is computed every cycle of the 50 Hz power signal. Therefore, when using Equations 2.3 and 2.4, the source impedance is actually kept constant for each P_{st} evaluation of 1-min. Therefore, the usage of an on-line Z_s value, does not change the fact that voltage variations due to the source-side are decoupled from the individual flicker contributions of the loads. The usage of online estimation procedure provides the variations of the source impedance that is not estimated by the utility, which might be due to the instantaneous upstream load changes. The utility, on the other hand, provides only two Z_s values, one for summer and one for winter load profiles. As a result, either Z_s estimation by the utility or Z_s computed on-line can be used for the proposed method depending on the design requirements.

CHAPTER 3

RESULTS FROM the PQ^+ ANALYZERS INSTALLED ON THE TURKISH ELECTRICITY TRANSMISSION SYSTEM

FC^M (Flicker Contribution Meter) developed throughout this thesis work is implemented on the PQ^+ Analyzers developed through the National Power Quality Project [16].

FC^M has the same hardware with the PQ^+ Analyzers. Hardware configuration of the PQ^+ Analyzer is illustrated in Figure 3.1. It is composed of a power supply unit, a signal conditioning unit, a data acquisition unit, a GPS module, a hard disk, an industrial mini ITX PC and an LCD display to demonstrate the power quality variables. It has a rack mount enclosure to be placed in cabinets in transformer substations. All the data processing is done on the mini ITX PC. Data acquisition is done with a signal conditioning unit and data acquisition unit. The time synchronization is achieved by the use of a GPS antenna and module. Time synchronization among the PQ^+ Analyzers is essential because for correct flicker contribution detection, synchronized measurements for each load current and voltage at the PCC is required as explained in Chapter 2. The hard disk is used to store the raw data or for collecting the data processed when the ADSL connection is out of service.

Connection diagram of the PQ^+ Analyzers to a substation is shown in Figure 3.2. FC^M uses the outputs of the voltage and current transformers at the substations. The output of the voltage transformer, whose rated value is 57V RMS line to neutral, directly drives the voltage input of the device. The outputs of the current transformers, on the other hand, in substations are usually in 5 A or 1 A range. This output is taken

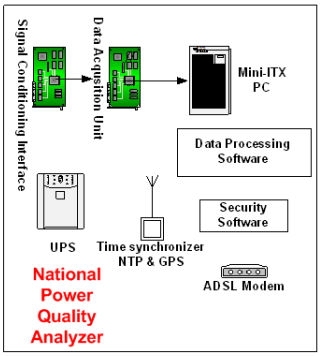

Figure 3.1: Power Quality Monitor hardware

by using toroidal current probes with no air gaps as shown in Figure 3.2. The ratio of these toroidal transformers are 2000/1 and the outputs of the toroidal probes drive the current inputs of the PQ^{+} Analyzer. Current input is then converted to a voltage signal with the signal conditioning unit.

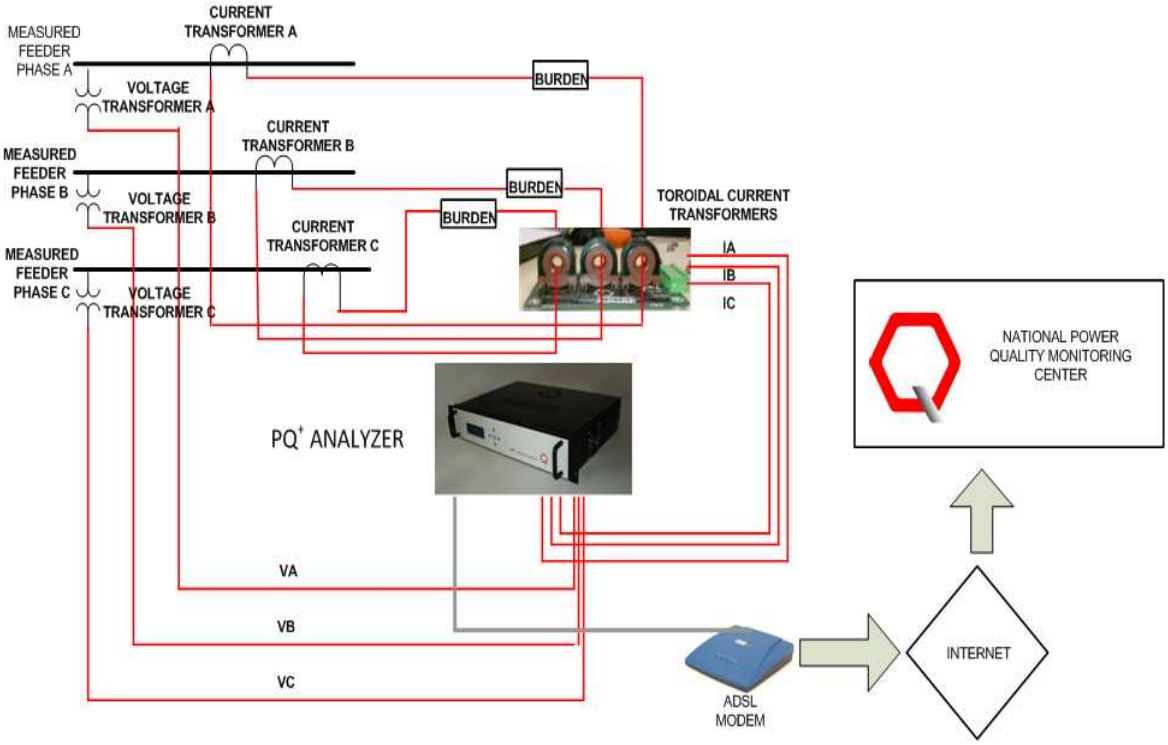

Figure 3.2: Connection diagram of the PQ^{+} Analyzer and hence the FC^{M}

The PQ^{+} Analyzers use the Fedora operating system. The software used to process

(a) PQ^{+} Analyzer components (b) cabinets for PQ^{+} Analyzers

Figure 3.3: PQ^{+} Analyzer components and the cabinets used for transformer substation installations

the power quality data on the device is written in the C language. Voltage and current waveforms for the three phases are sampled at 25.6 kHz/channel (512 samples/cycle for 50 Hz signal) and these waveforms are buffered at every 3-sec windows. These 3-sec buffers (76800 samples/channel) are processed to obtain instantaneous flicker level (IFL) values and the results are used to make the statistical computation of 10-min flicker. The schematic diagram the FC^{M} analysis software is given in Figure 3.4.

The results to be presented in this chapter from now on are collected from three different transformer substations in Region-13 of the Turkish Electricity Transmission System. It is the part of the system located in the mid-south of the country. There are a number of intermittent current demanding consumers in this region such as scrap metal iron and steel plants, blast furnace integrated iron and steel plants, rolling mills, cement factories and other industrial plants.

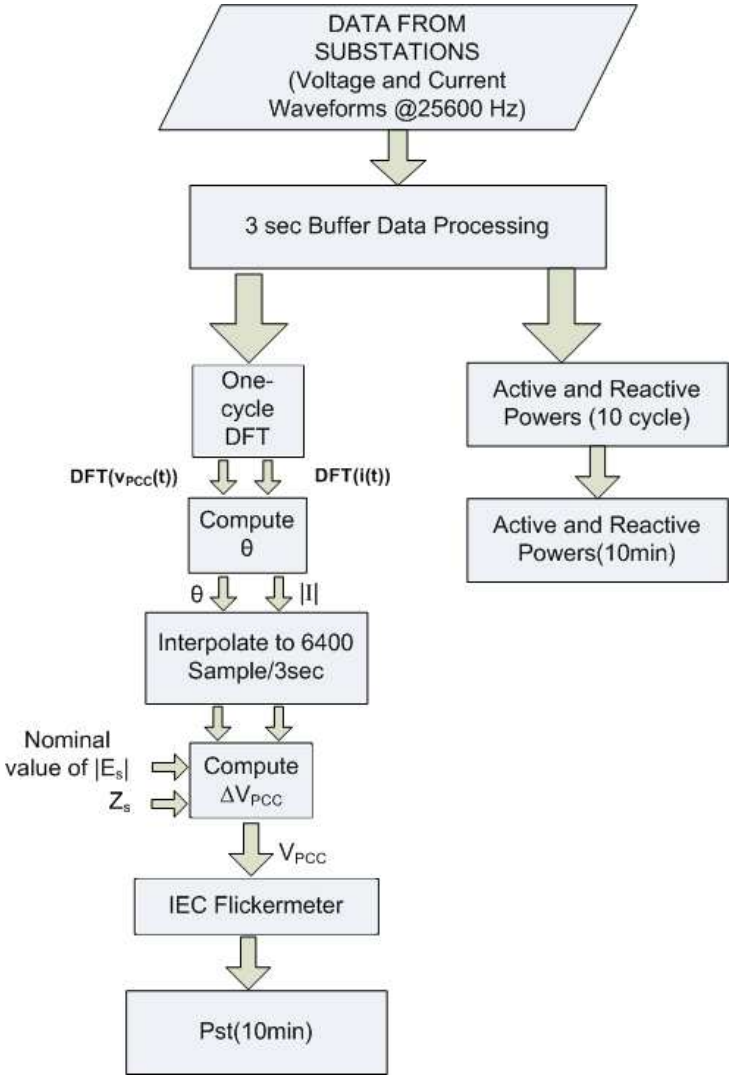

Figure 3.4: Block diagram of FC^M analysis software.

3.1 RESULTS FROM ISKENDERUN-2 SUBSTATION

The investigated transformer substation in Region-13 is already given in Section 2 in the model verification part. The part of the transmission system under investigation is given in Figure 2.1 and the corresponding single line diagram is given in Figure 2.2. These figures are repeated as Figures 3.5 and 3.6 for the convenience of the readers here.

The active and reactive power consumptions of the feeders given in Figure 3.6 are

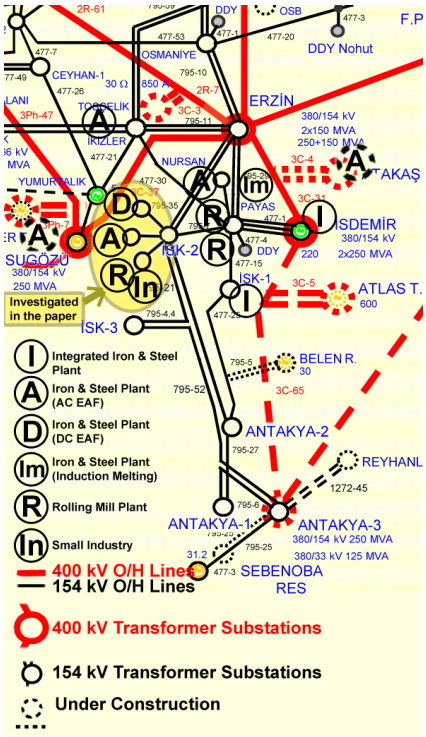

Figure 3.5: Connections of part of the Turkish transmission system

computed and plotted as 1-min averaged values. Total power demand and current consumption of the loads, D, A, and R+In, are calculated by summing up synchronous current measurements at the measurement points denoted by MP_1, MP_2, and MP_3. Total active and reactive power variations of the loads at the PCC are given in Fig 3.7(a). Fig 3.7(b) shows the total flicker contribution of the loads, D, A, R+In, at the PCC by using the complete model ($R_s I \cos\theta + X_s I \sin\theta$), together with time-varying source parameters. IEC flickermeter measurement is also plotted in Figure 3.7(b) for comparison purposes. A comparison between the flicker contribution of the interconnected system in Figure 2.4 in Chapter 2 with the flicker contribution of all loads given in Figure 3.7(b) shows that, only in approximately half of the measurement period, flicker contribution of the loads is dominant.

For example, during the first 60 minutes of the measurement period, flicker contribution of loads is too low, because in that period Plant A containing AC EAFs is not operating, and total P and Q consumptions are relatively low when compared with the recorded maximum demand values. Flicker contributions of the individual loads A,

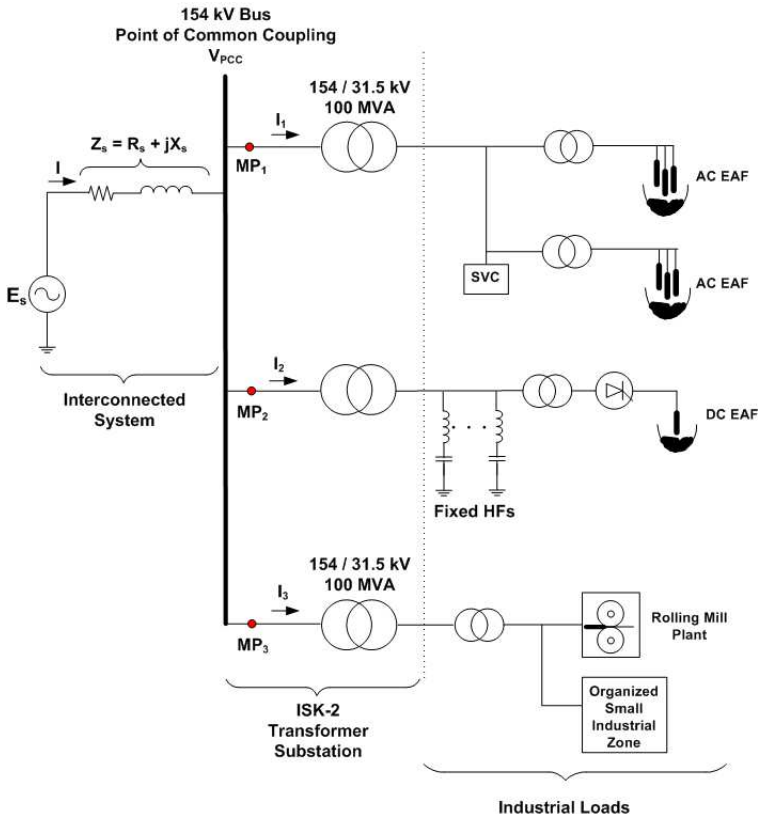

Figure 3.6: Simplified single-line diagram of ISKENDERUN-2 transformer substation

D, and R+In are also computed by using the FC^Ms. Power demands and flicker contributions of loads A, D, and R+In, are as given in Figures, 3.8(b), 3.9(b) and 3.10(b), respectively. FC^Ms are programmed to use the simplified model with time-varying X_s for this experiment. In order to be able make a decision, whether the simplified model with time varying X_s can give accurate results or not, their measurements are compared with the reference case. Reference case is the output of the FC^M employing complete model with time-varying Z_s, for each load. Reference cases are also plotted on the same Figures. It is observed from Figures 3.8(b), 3.9(b) and 3.10(b) that the simplified model with time-varying X_s gives quite accurate results in comparison with complete model with time-varying X_s. Therefore, from now on, simplified model will be employed in the proposed FC^M. On the other hand, the use of time-varying X_s is impractical for many cases. This is because, before making flicker contribution computations by the FC^M, a series of measurements and computations at the PCC are to be carried out in order to estimate the time-varying X_s as described in Chapter 2.

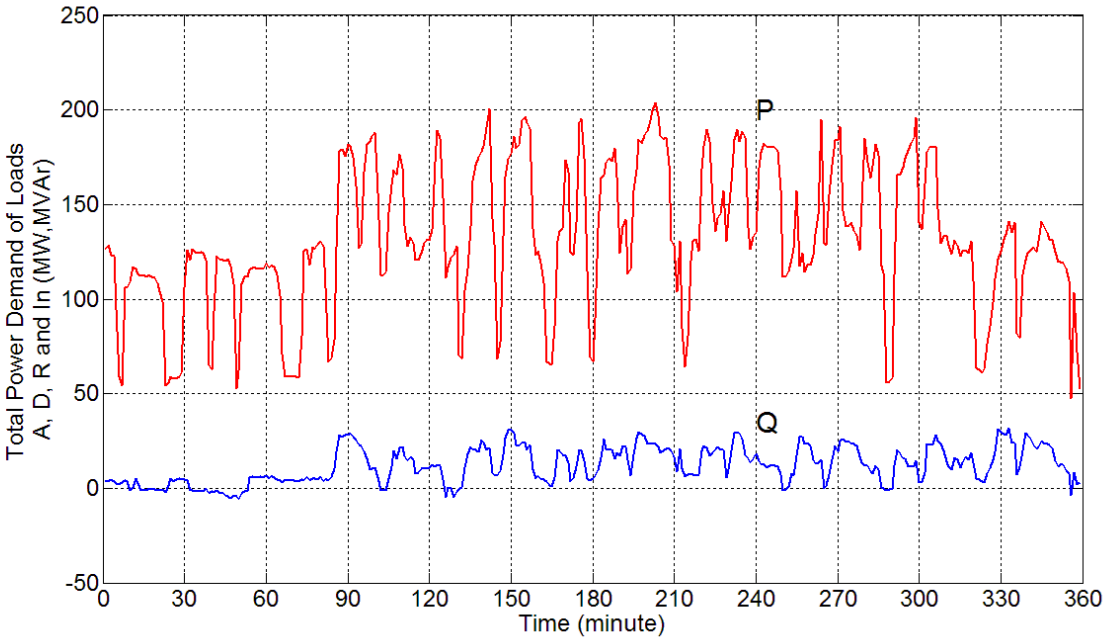

(a) The total active and reactive power demands of the loads

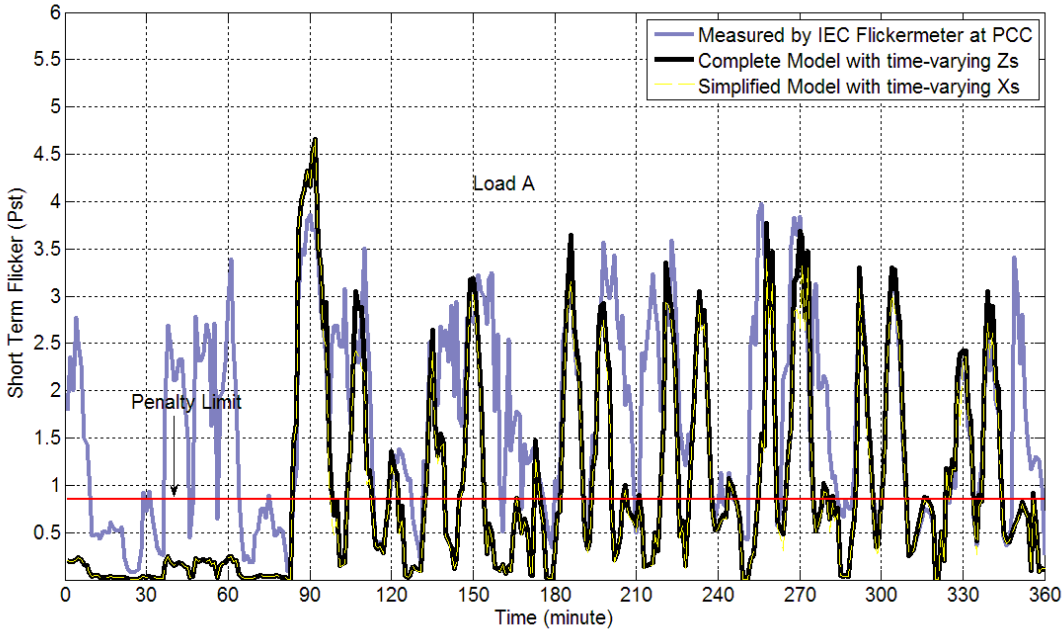

(b) Calculated flicker contributions of all the loads (D, A, and R+In)

Figure 3.7: Total Power Demand and Flicker Contribution of Plants

However, the use of a constant value for X_s, determined by running PSS/E program for the measurement day, is very practical only if the interconnected system is widely

monitored by a SCADA system. Therefore, flicker contributions of the loads, A, D and R+In, determined by using the constant value of the X_s mentioned above are to be compared with the FC^M measurements based on time-varying X_s. These comparisons are given in Figs 3.11, 3.12 and 3.13 respectively for loads, A, D, and $R + In$. As can be observed from these Figures, FC^M measurements with constant X_s, are almost the same with those with time varying X_s. It can therefore be recommended that the FC^M is programmed with the simplified model employing constant X_s value ($X_s I \sin\theta$) in order to make the FC^M practicable with sufficient accuracy. Note that $I \sin\theta$ is the individual reactive current component of the loads.

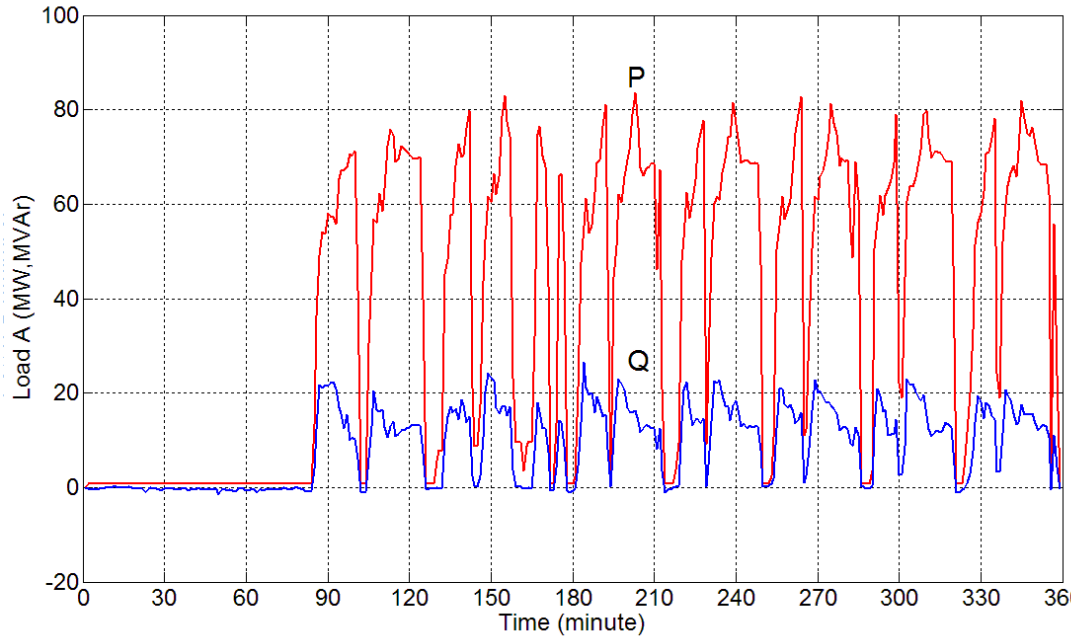

(a) Power demand of load A.

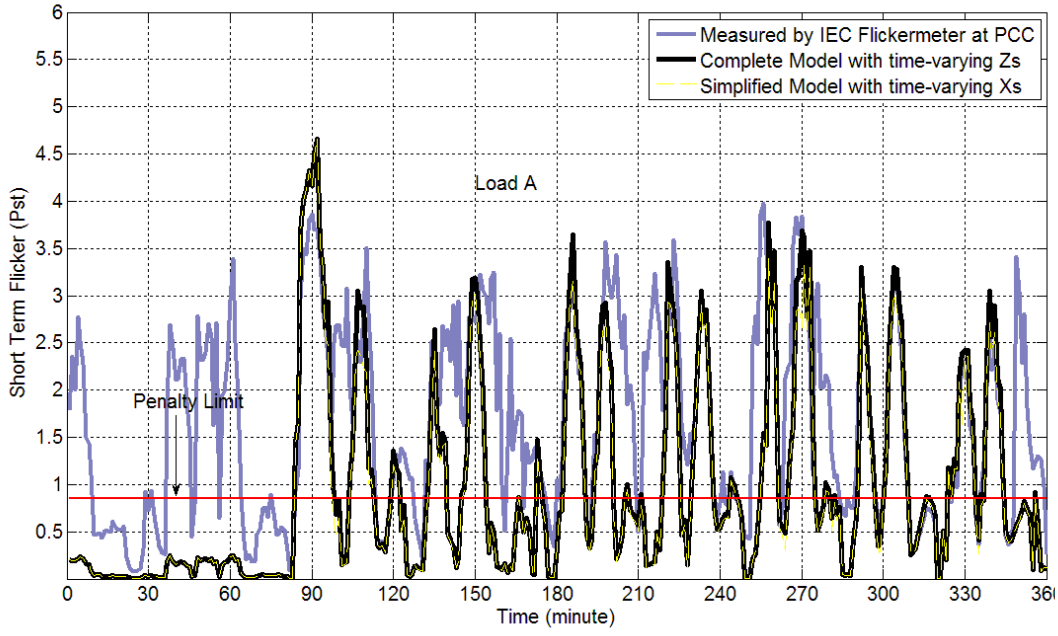

(b) Flicker contribution of load A computed with complete model and simplified model with time-varying source parameters.

Figure 3.8: Flicker Contribution of Plant A.

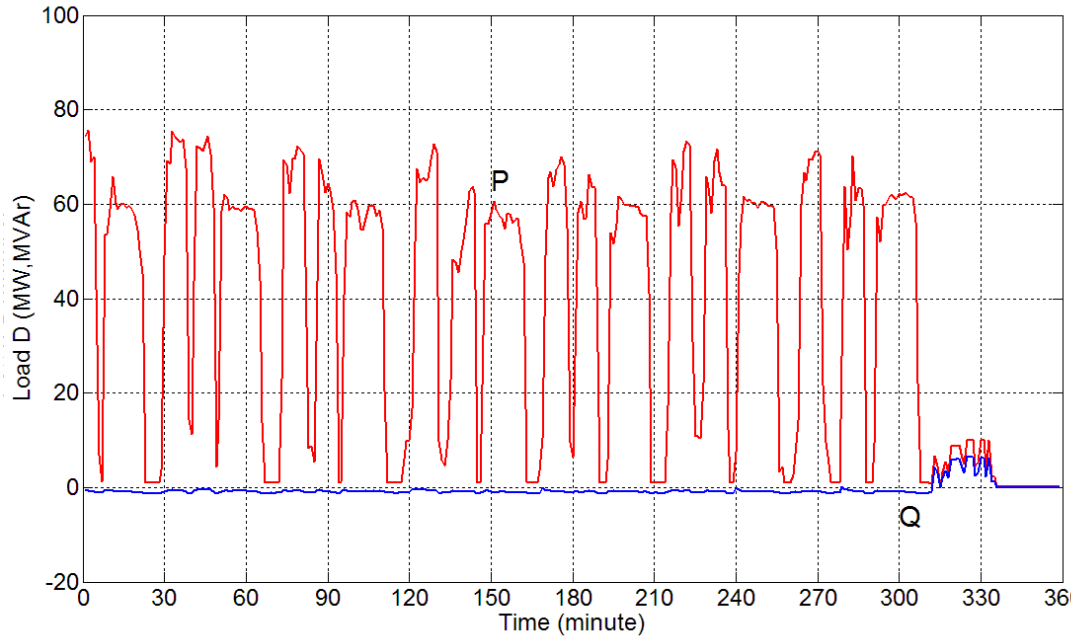

(a) Power demand of load D.

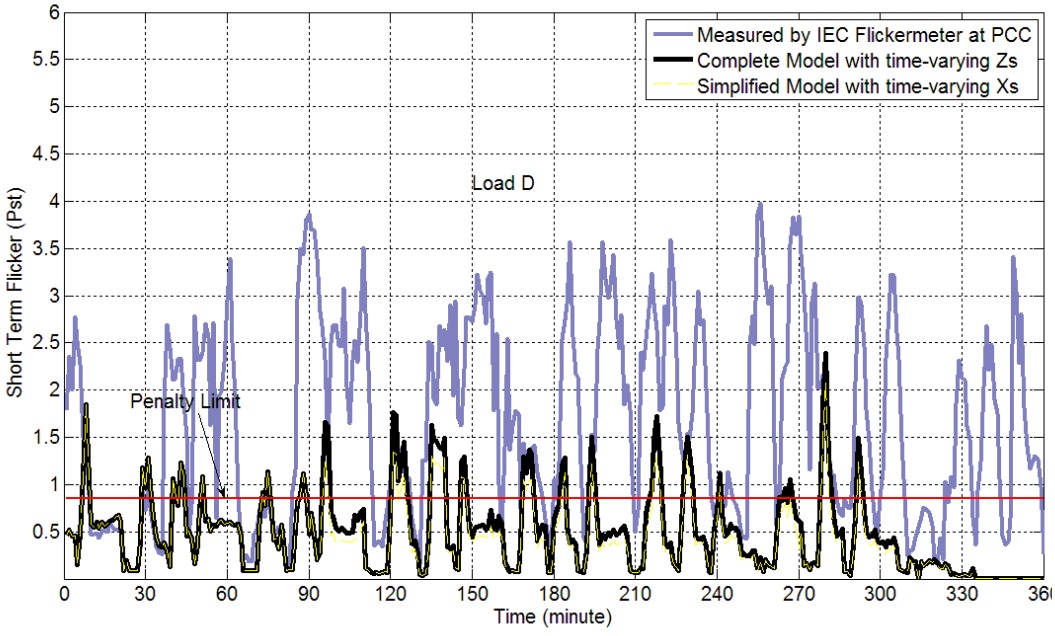

(b) Flicker contribution of load D computed with complete model and simplified model with time-varying source parameters.

Figure 3.9: Flicker Contribution of Plant D.

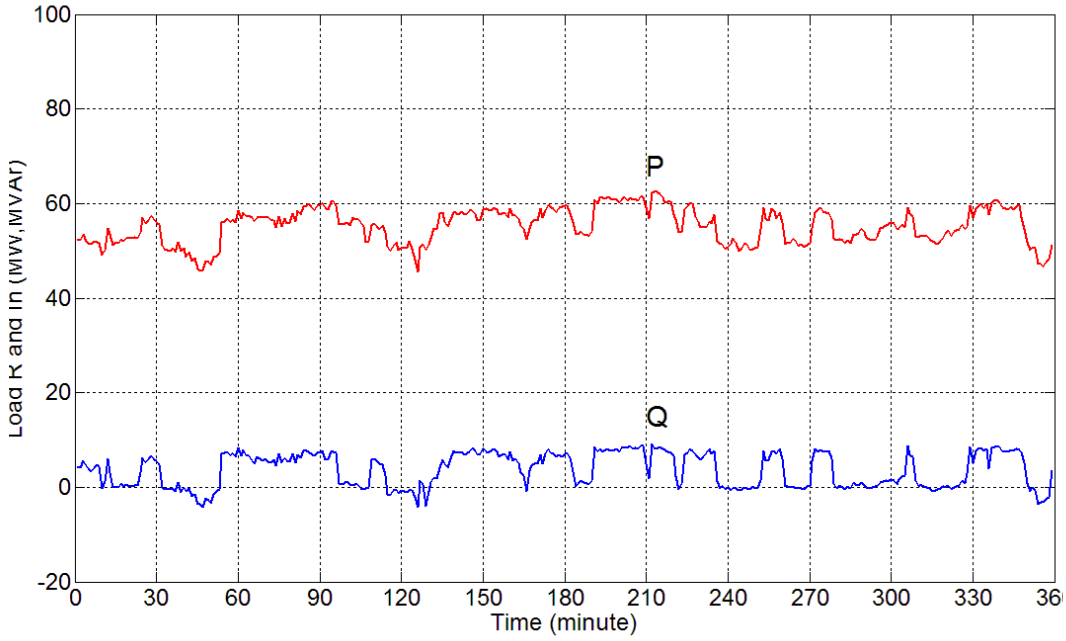

(a) Power demand of load $R + In$.

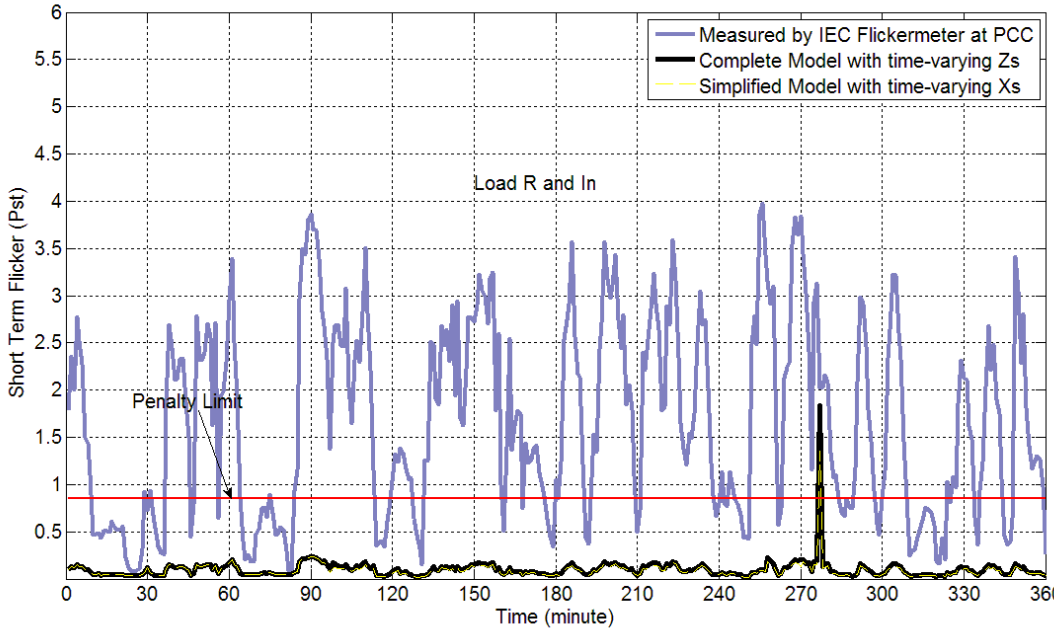

(b) Flicker contribution of load R and In computed with complete model and simplified model with time-varying source parameters.

Figure 3.10: Flicker Contribution of Plant R and In.

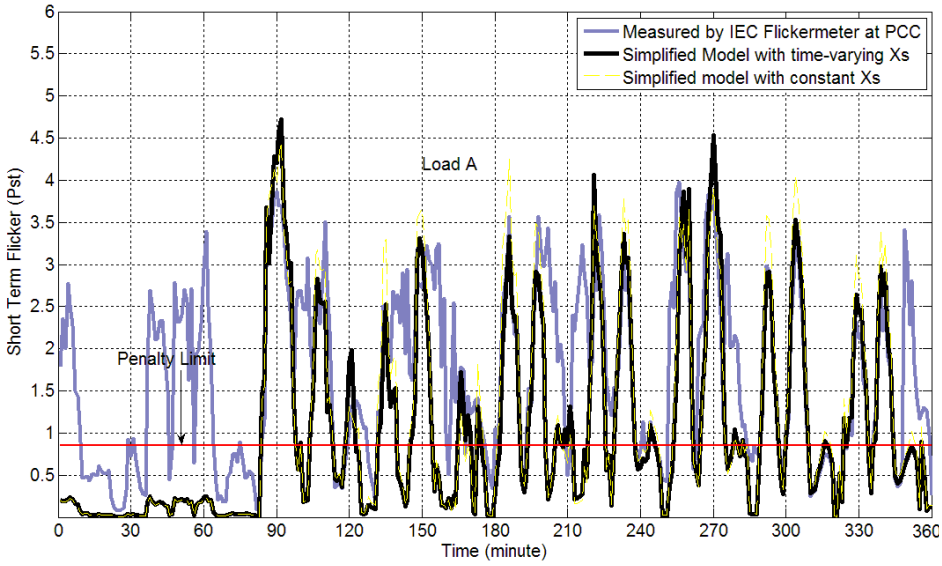

Figure 3.11: Flicker contribution of the load A to the PCC measured by the proposed FC^M with simplified model and both time varying and constant X_s.

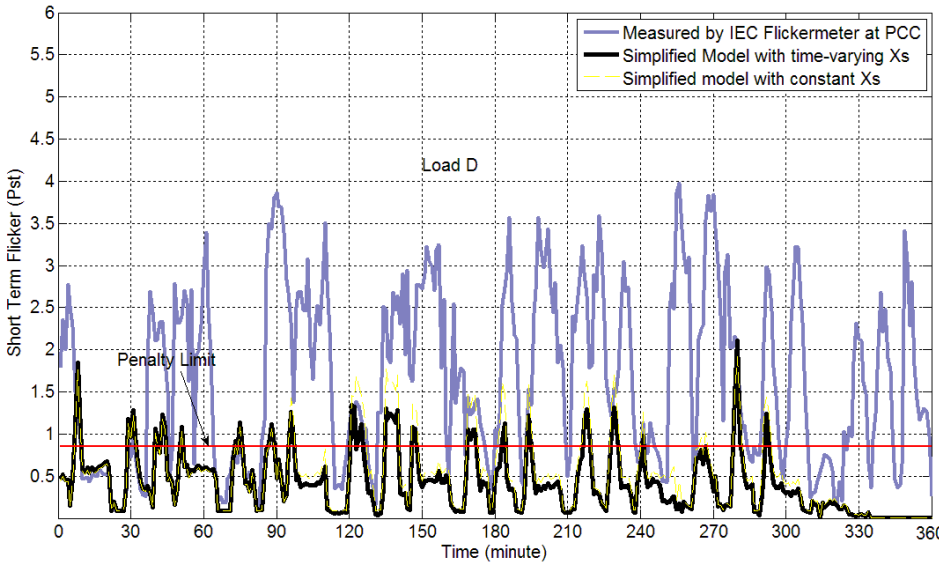

Figure 3.12: Flicker contribution of the load D to the PCC measured by the proposed FC^M with simplified model and both time varying and constant X_s.

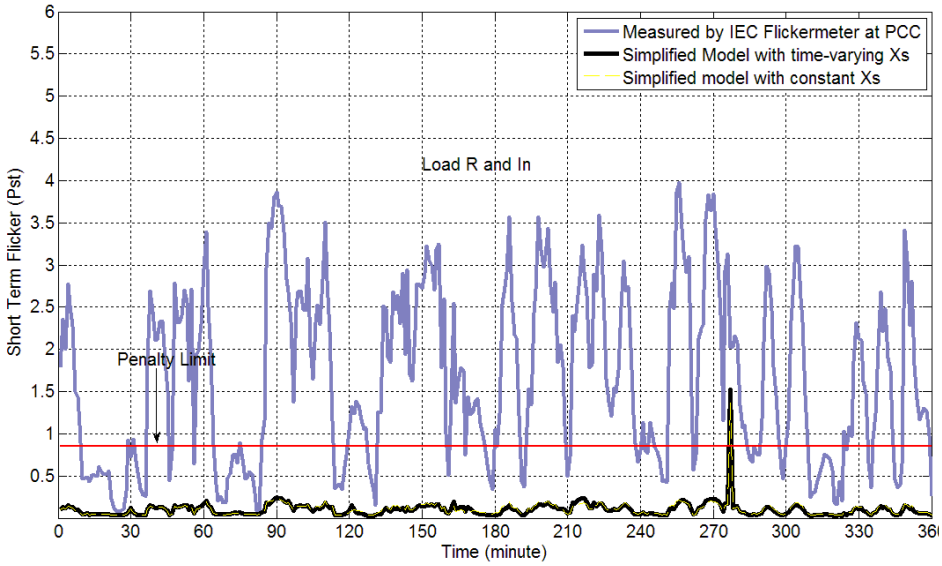

Figure 3.13: Flicker contribution of the load R and In to the PCC measured by the proposed FC^M with simplified model and both time varying and constant X_s.

3.2 RESULTS FROM PAYAS SUBSTATION

The investigated part of the transmission system is given in Figure 3.5. In the investigated substation Payas, there is a scrap metal iron and steel factory and feeders supplying the rolling mill plants of an iron and steel factory, connected to 154 kV busbar. Also there is an induction furnace connected to medium voltage level together with the urban loads as given in Figure 3.14. Figures 3.14, 3.15, 3.16 show the measurement points, power demand of the loads and flicker contribution of the plants, respectively.

Measurement points are shown by MP_1 and MP_2 in Figure 3.14. FC_1^M at MP_1 takes voltage measurements at the PCC and total current measurements of the induction furnace and plant, industry load and urban loads. The FC_2^M at MP_2 takes the current measurement of the induction furnace load as given in Figure 3.14. The contribution of this induction furnace is investigated in this section.

The short circuit current is given as 10206.9 A at high voltage level by the utility and using this value the system impedance at 31.5 kV level is determined to be X_s = 3.075Ω (seen from MP_1 towards TR.A), which energizes the medium voltage level with a 50 MVA power transformer with a short circuit voltage value of U_k = 13.672% .

It can be observed in Figure 3.16 that for the total measurement period of approximately 13 hours, the flicker measured at the PCC by the IEC flickermeter at MP_1 is above the flicker limits defined by the regulations for a significant ratio of the total measurement period. The loads connected to the PCC are the induction furnace plant, and urban and industrial loads which are not main flicker contributors due to their natures. Therefore, it is expected that the flicker at the PCC (MP_1) in Figure 3.16 receives flicker from the high voltage side of TR.A. This is also observed from the results obtained using the FC_2^M connected to MP_2. The induction furnace plant is the highest probable flicker source among the other load types supplied from the PCC at MP_1. As given in Figure 3.16, the flicker contribution of the induction furnace plant measured by the FC_2^M at MP_2 is much lower than the flicker measured at MP_1. Therefore it can be concluded that the flicker at the PCC (MP_1) is mainly due to the

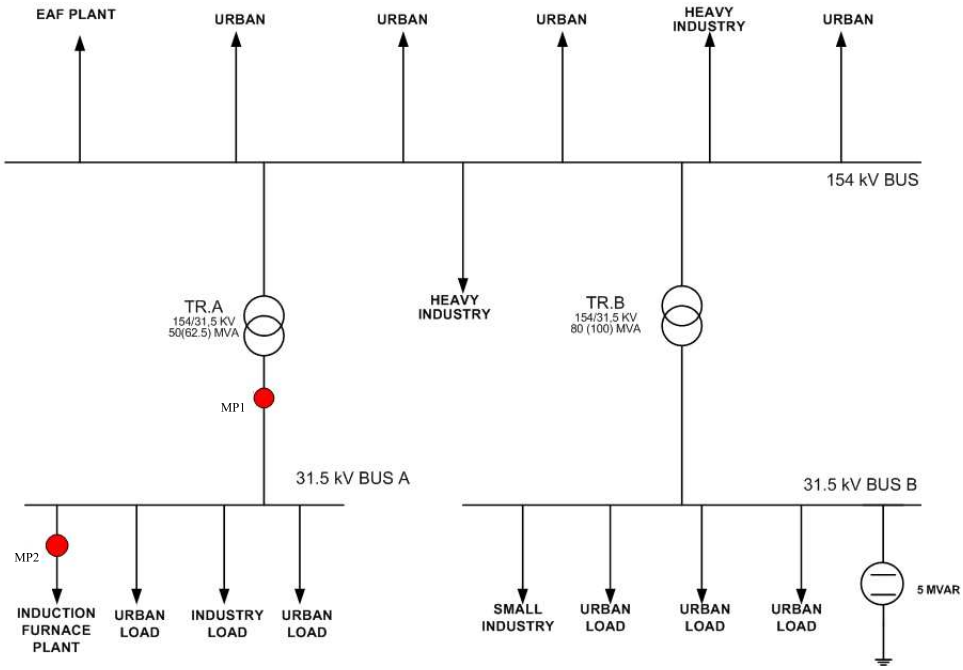

Figure 3.14: Single line diagram of the case study for induction furnace load.

source side, which is the high voltage side (154 kV) of the transformer TR.A. This is an expected result, because as observed in Figure 3.14, an EAF plant is supplied directly from the 154 kV bus and the flicker it causes has a downstream effect on TR.A towards the PCC(MP_1).

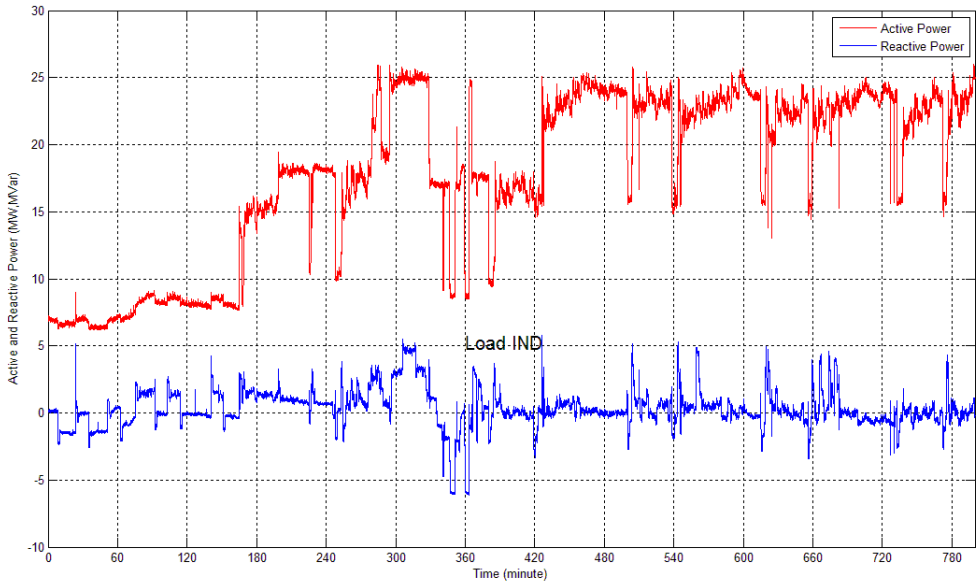

Figure 3.15: The active and reactive power demand of the induction furnace load given in Figure 3.14.

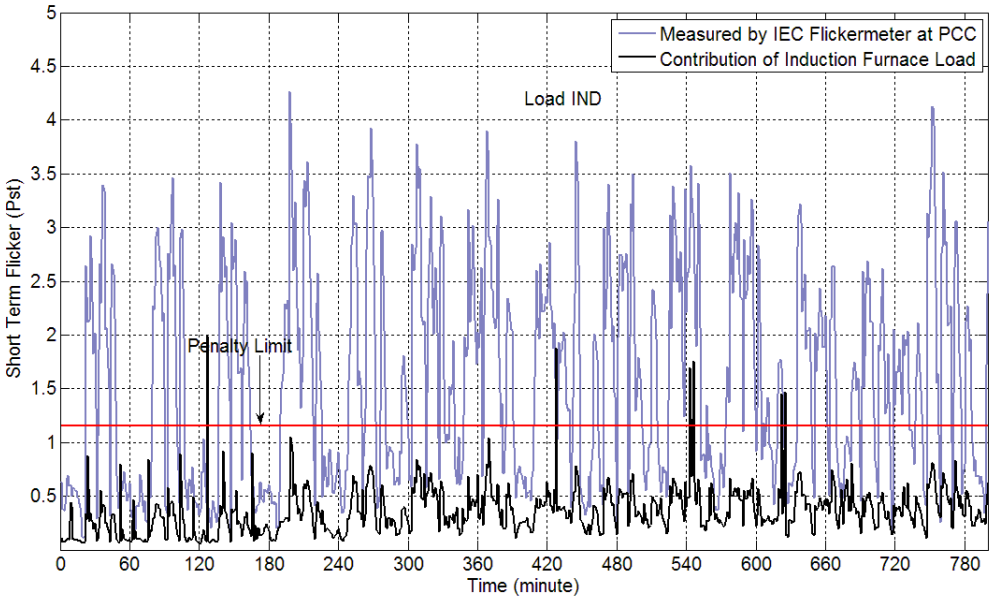

Figure 3.16: The flicker contribution of induction furnace plant given in Figure 3.14.

3.3 RESULTS FROM ISDEMIR SUBSTATION

The investigated part of the transmission system is given in Figure 3.5. In the integrated iron and steel factory ISDEMIR, there is a blast furnace iron and steel plant, feeders supplying hot rolling mill plants and oxygen producing facilities, a feeder supplying 4 ladle furnaces, and combined natural gas power plants. Under normal operating conditions, power plants and the hot rolling mill feeders are supplied from the same 154 kV PCC. The plant under investigation has power demand from Erzin by an overhead transmission line and Payas substation 500 m away from its facilities. The ladle furnaces are supplied from Payas substation and other facilities' power demand are supplied from both Erzin substation and the power generators of the plant itself. The single line diagram of the ISDEMIR transformer substation is shown in Figure 3.17. Hatay feeder at the top right of Figure 3.17 is not energized in this case.

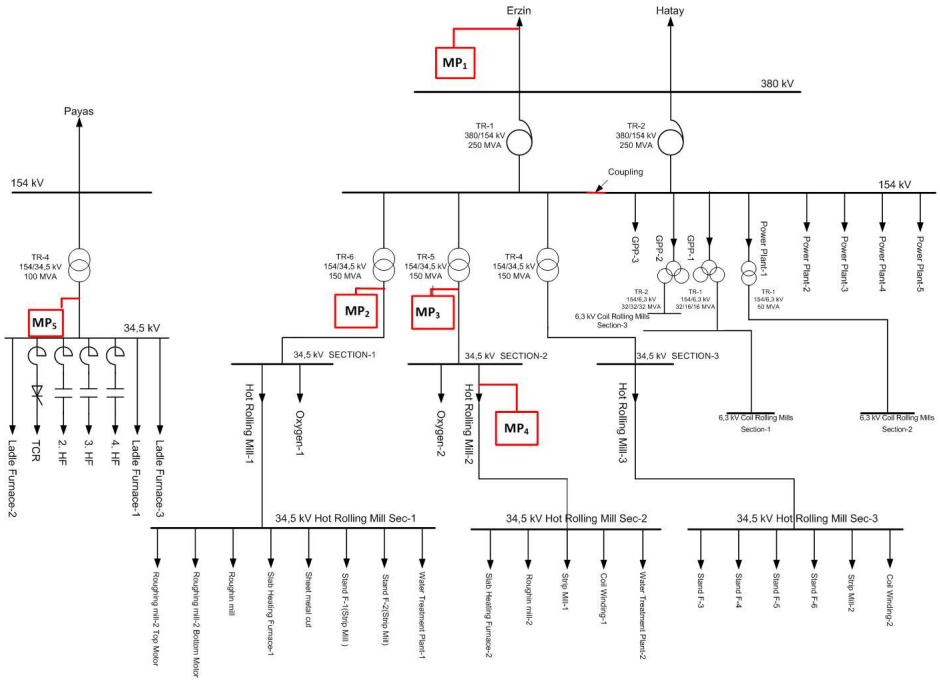

Figure 3.17: Single line diagram of the case study for ISDEMIR transformer substation.

Measurement points are shown by MP_1 to MP_5 in Figure 3.17. MP_1 takes voltage measurements at the 380 kV PCC and the total current drawn by the integrated iron and steel factory from Erzin feeder. FC_2^M at MP_2 and FC_3^M at MP_3 takes the voltage

and current measurements of the hot rolling mill plus the oxygen producing facilities. The hot rolling mill and oxygen facilities are supplied by 3 different sections connected to the 34.5 kV secondary sides of the power transformers. The first two sections are the major intermittent loads with higher VA ratings. Therefore, in order to investigate the flicker contributions of the facility, these feeders are measured. Moreover, a measurement at MP_4 is also carried out to analyze the flicker characteristic of the hot rolling mill plant. Another measurement is achieved at MP_5 to investigate the effect of the ladle furnace. During the measurements, the periods in which the intermittent loads of the facility (hot rolling mill plant) do not operate is also analyzed to make a comparison. The power demand for each measurement point is given in addition to the flicker contributions of loads in Figures 3.18, 3.20, 3.21, 3.22 and 3.23.

The short circuit current values provided by the system operator, for the ISDEMIR 380 kV PCC are tabulated in Table 3.1 with the $\frac{X}{R} = 6.875$ given for this bus.

Table 3.1: The Short Circuit Current Values Given by the System Operator for ISDEMIR 380 kV Bus

2010 Minimum Load	8.49 kA
2010 Summer Peak Load	10.78 kA

It is observed in Figure 3.18 that, despite the fact that contribution of the integrated iron and steel factory is very low, the flicker measured at the PCC is above the limits defined by the regulations. Therefore it can be concluded that the source side effects have a major role determining the flicker level at the 380 kV PCC. this effect is also observed at the 34.5 kV bus when same analysis is achieved at MP_2. This shows the propagation of the flicker effect from the 380 kV busbar towards the medium voltage busbars. The result of the analysis at MP_2 compared with the results at MP_1 are shown in Figure 3.19.

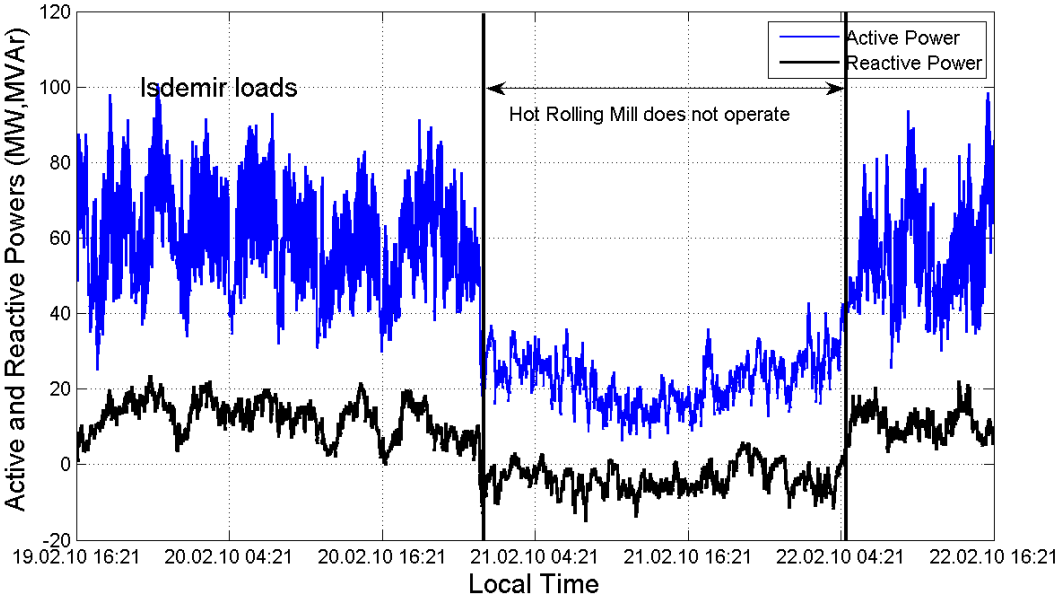

(a) Power demand of integrated iron and steel factory, ISDEMIR, measured at MP_1.

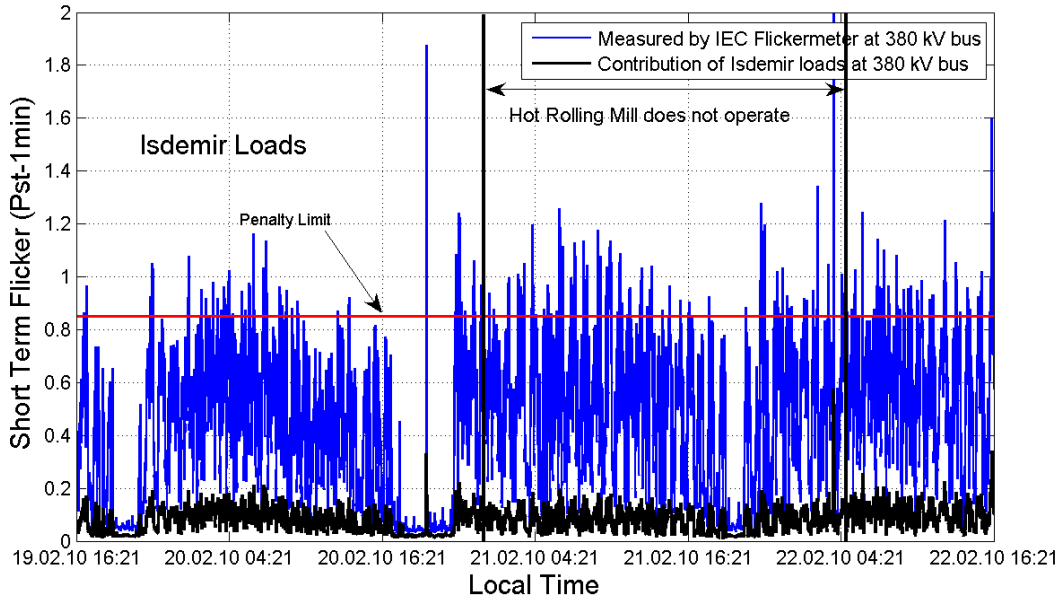

(b) Computed flicker contribution of integrated iron and steel factory loads from MP_1.

Figure 3.18: Flicker contribution of integrated iron and steel factory, ISDEMIR.

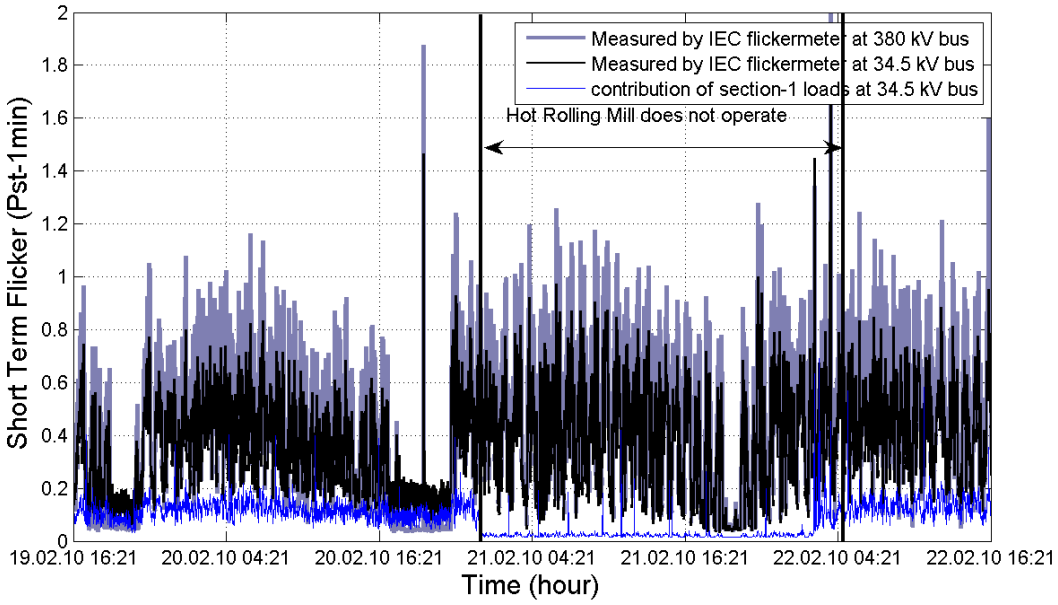

Figure 3.19: Propagation of the flicker effect from 380 kV busbar towards 34.5 kV busbar.

It is worth to note that, there are multiple iron and steel plants whose operation is based on arc furnaces, exist in the vicinity of the investigated facility. Although these arc furnace plants are not directly connected to the 380 kV PCC, the deterioration in the voltage caused by these plants may spread to higher voltage level busbars through the autotransformers, power transformers and transmission lines due to the interconnected structure of the grid [12]. Erzin feeder, which is supplying the power demand of the investigated facility is connected to the transformer substations Iskenderun-2 and Payas at 154 kV level. These substations, which are also investigated in Sections 3.1 and 3.3 supply power to two AC EAFs, one DC EAF and one induction furnace. Hence the flicker that already exists in the 154 kV bus is likely to be observed at the 380 kV bus.

The flicker values measured at the 34.5 kV bus by the IEC flickermeter at MP_2 and MP_3 are above the flicker limits defined by the regulations for a significant ratio of the total measurement period. It is obvious that the flicker contribution of only these sections are under the limitations as can be observed from Figures 3.20 and 3.21. The flicker at the 380 kV bus has a downstream effect on 34.5 kV bus through the

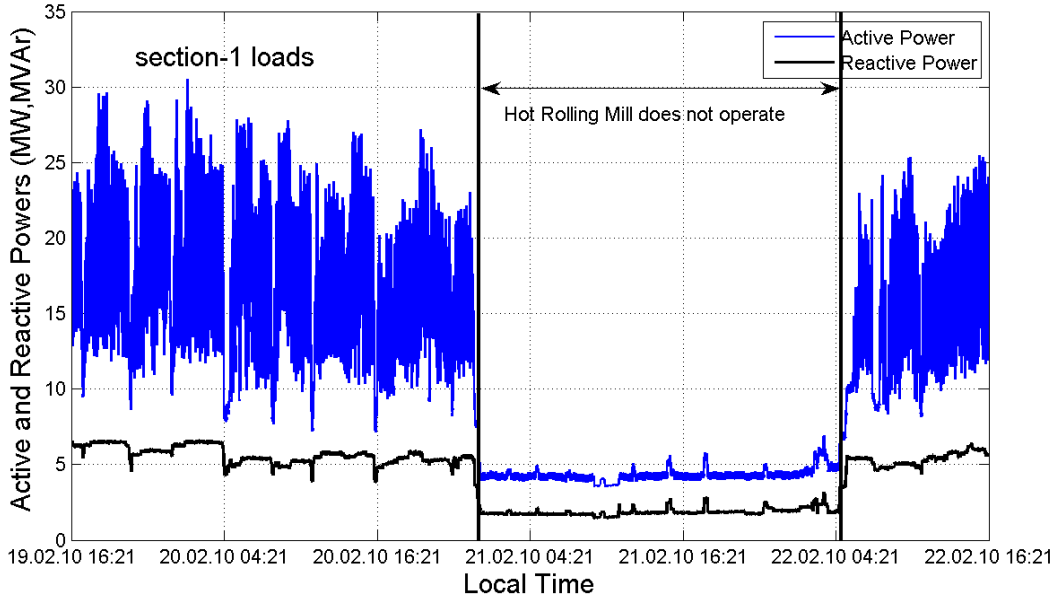

(a) Total power demand of hot rolling mill and oxygen facility section-1(MP_2).

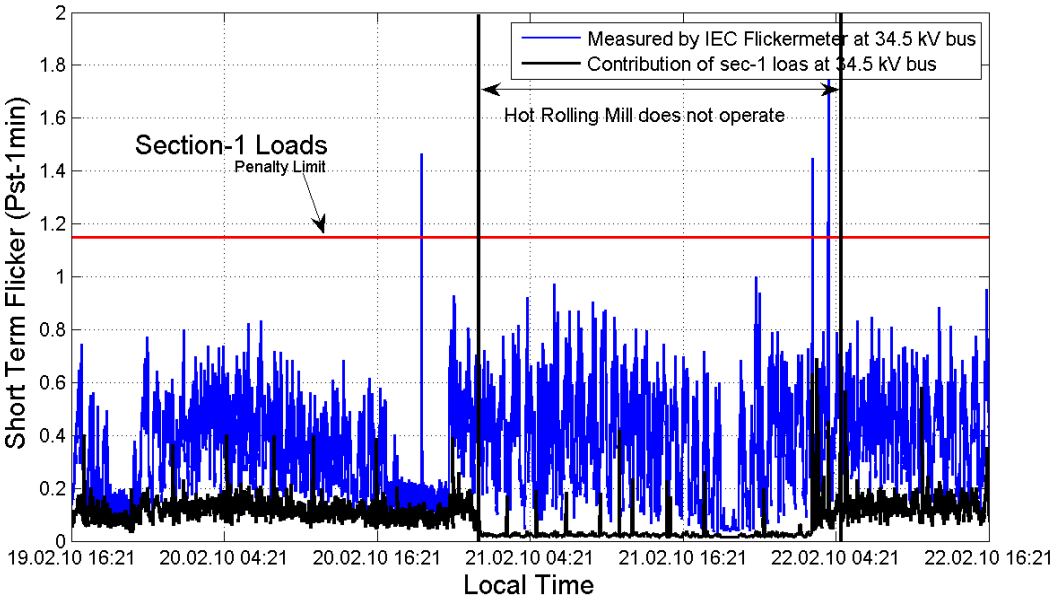

(b) Computed flicker contribution of hot rolling mill and oxygen facility section-1 (MP_2).

Figure 3.20: Flicker contribution of hot rolling mill and oxygen facility section-1.

autotransformers and transformer 5 and 6 (TR5 and TR6). This downstream effect is also verified by looking at the periods where the hot rolling mill plant does not operate. Even under these circumstances, flicker at the bus is above the limits which implies that the flicker is due to the source voltage variations.

In Figure 3.22, the flicker contribution of one of the hot rolling mill feeder is investigated alone.

The flicker contribution of the ladle furnace which is connected to Payas substation through a power transformer of 100 MVA with $U_k = 10.4\%$ is shown in Figure 3.23. Even though it is equipped with an SVC system, it is observed that the contribution of the ladle furnace exceeds the limit for certain times at the 34.5 kV bus. The IEC flickermeter's reading is much above the limits due to the source side effects as mentioned earlier.

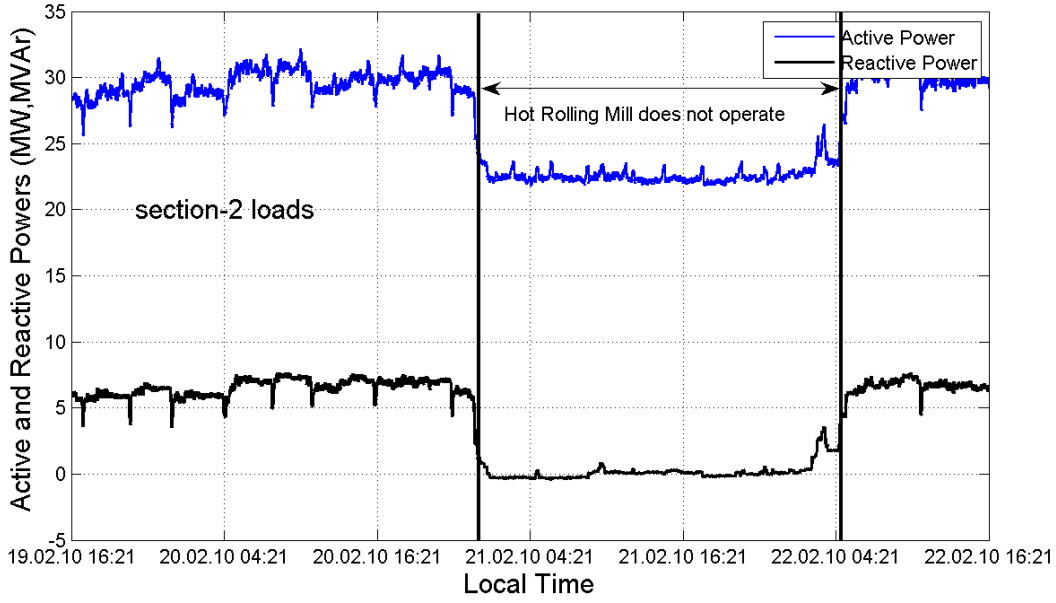

(a) Total power demand of hot rolling mill and oxygen facility section-2 (MP_3).

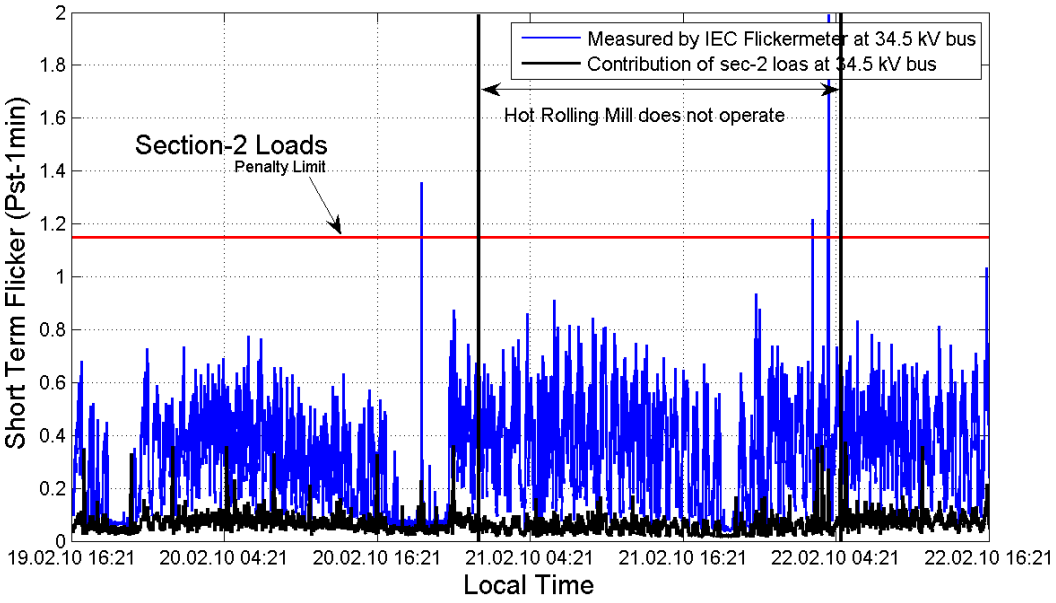

(b) Computed flicker contribution of hot rolling mill and oxygen facility section-1 (MP_3).

Figure 3.21: Flicker contribution of hot rolling mill and oxygen facility section-2.

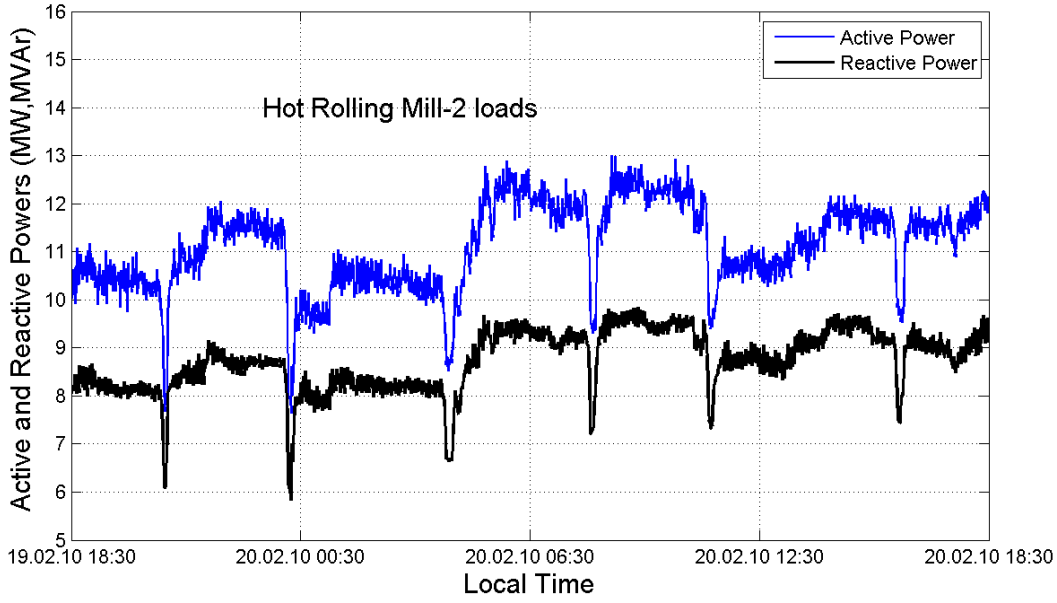

(a) Power demand of hot rolling mill-2 (MP_4).

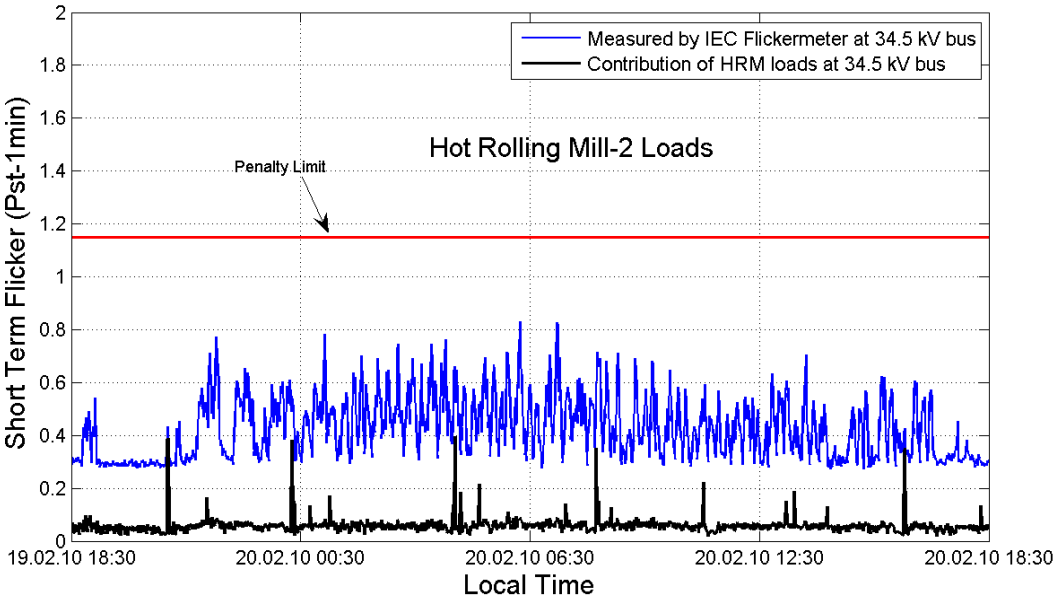

(b) Computed flicker contribution of hot rolling mill-2 (MP_4).

Figure 3.22: Flicker contribution of hot rolling mill-2.

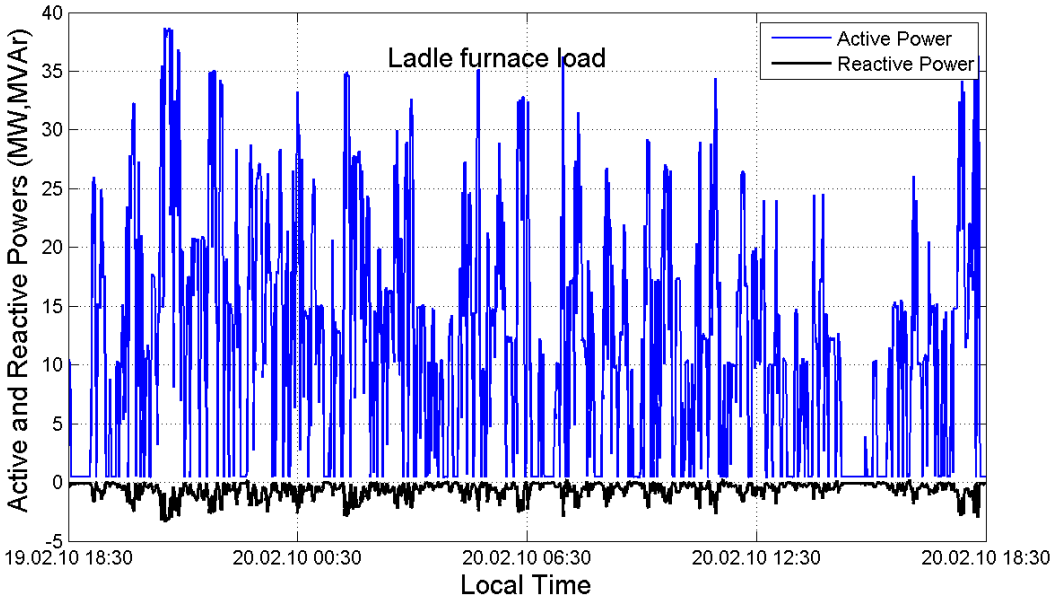

(a) Power demand of ladle furnaces 1,2 and 3 (MP_5).

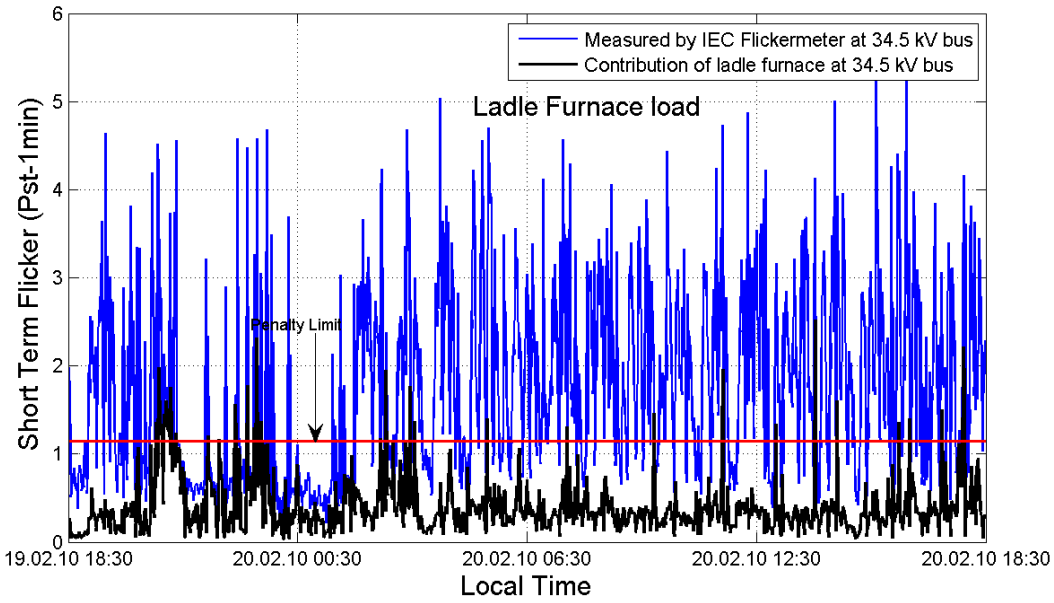

(b) Computed flicker contribution of ladle furnaces ladle furnaces 1,2 and 3 (MP_5).

Figure 3.23: Flicker contribution of ladle furnace.

CHAPTER 4

RECOMMENDATIONS ON THE APPLICATION OF THE FLICKERMETER STANDARD IEC 61000-4-15 BASED ON THE FC^M USAGE

Some further conclusions can be drawn from the results presented in Chapter 3. It has been observed that iron and steel plants especially the ones including AC EAFs, are the major sources of flicker, even though they are furnished with Static VAr Compensator (SVC) type flicker compensation systems. For most of the time, the flicker measured at the PCC where they are supplied exceeds the penalty limits defined by the regulations. Detailed research on the SVC type flicker compensation systems of the arc furnaces, have shown that although they compensate reactive power consumption of the plant, they are not always the best solution to mitigate the flicker problem. It has been found that these kind of compensators may amplify the interharmonics, especially the first one which is between the fundamental and the second harmonics, and hence may amplify the flicker caused by the plant [19]. Flicker contributions of DC EAFs are much smaller than those of AC EAFs. Their flicker levels can be kept below the penalty limits, by carefully designing the reactive power compensation system. Flicker contribution of the combination of continuous rolling mill shop and organized small industrial zone are found to be much below the penalty limit, for almost the whole measurement period.

In a point of common coupling there can be several cases when different combinations of plants are taken into account. Some of these several cases are: Only one of the plants may be exceeding the flicker limit, more than one plant may be exceeding the limit or all of the plants may be exceeding the limit. However due to the fact

that there are infinitely many phase combinations of the load currents, exceeding the flicker limit of one of the sources does not mean that the voltage at the PCC will lead to a flicker value exceeding the limit. The currents of the loads may be canceling the flicker effect of each other at the PCC partly or totally. Therefore understanding these cases with the IEC flickermeter can not always be easy in practice.

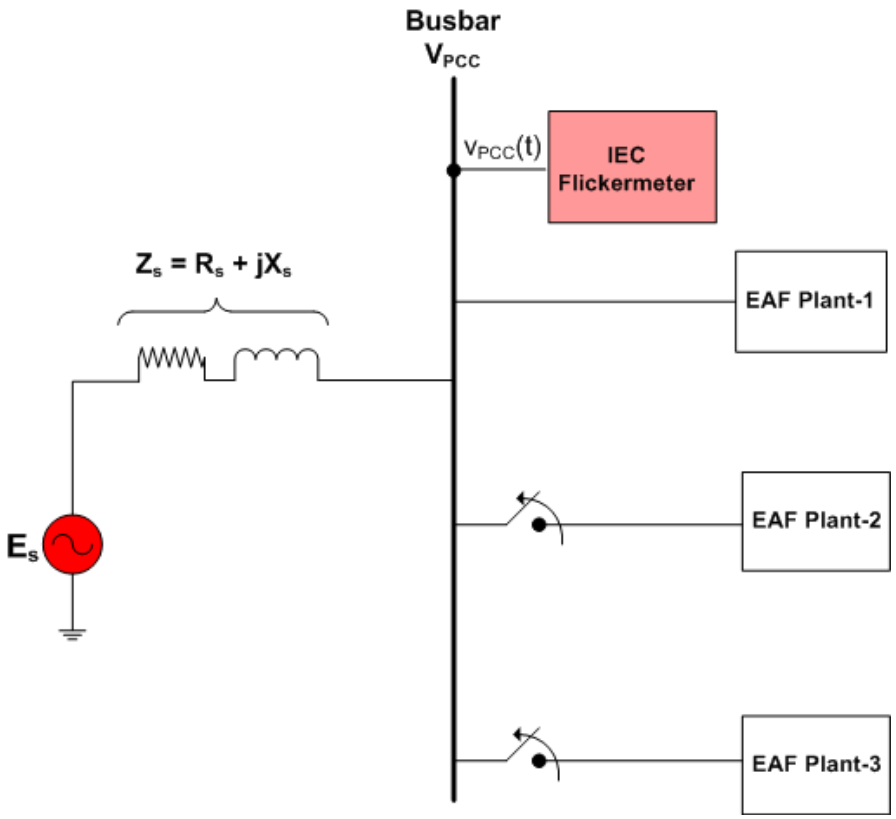

Figure 4.1: A possible configuration with IEC flickermeter to determine the flicker contribution of EAF plant-1

In Figure 4.1 one possible solution to determine the flicker contribution of each load is shown. IEC Flickermeter connected to the busbar measures the flicker caused by Plant-1 in addition to the flicker effect coming from the source side, E_s. One drawback of this method is that it is not always possible to stop the operation of the other plants. The other drawback is that background effect of the source, E_s is also included in the measured flicker level and hence the IEC flickermeter still does not show flicker caused by ”only” Plant-1. Therefore this approach seems impractical for identifying the contribution of a single plant. The utilization of FC^Ms to identify the individual

flicker contributions of the plants may be a solution to the problem. Investigating the results obtained by FC^Ms may lead to several different cases and for each case different countermeasures can be taken. Below is provided a list of these possible cases:

CASE-1 The configuration for Case-1 is given in Figure 4.2(a). FC^Ms are connected to measure the individual load currents of all three plants and one IEC flickermeter is connected at the PCC. Assume that all FC^Ms and the IEC flickermeter measure flicker contributions above the defined limits as shown in Figure 4.2(a). Two solutions can be recommended in this case:

Solution-1: Each plant takes its own countermeasure to reduce its flicker contribution and hence the flicker at the PCC is reduced.

Solution-2: A single flicker compensation system is installed at the PCC. The cost can be divided among the plants supplied from the PCC and the utility proportional to the P_{st} values measured by the FC^Ms. This solution is illustrated in Figure 4.2(b).

CASE-2 Two of the FC^Ms measure flicker above the permitted limits defined by the regulations as given in Figure 4.3. In this case one solution might be that each plant takes its own countermeasure to result in reduced flicker at the PCC. A second solution might be installing a single flicker compensation system at the PCC. Similar to solution 2 of Case-1, the cost may be divided among the plants that exceed the limit proportional to the P_{st} values measured by the FC^Ms .

CASE-3 In this case, none of the FC^Ms measure flicker above the permitted limits defined by the regulations; however, IEC flickermeter at the PCC measures flicker above the limit. In this case, flicker comes from the utility side plus the combined effect of the plants. The combined effect of the loads can either eliminate or strengthen one another depending on the relative phases of the load currents. The configuration is shown in Figure 4.4.

In this case utility should anticipate the results of such a connection before letting the plants construct their EAFs or ladle furnaces with such a capacity and supply them.

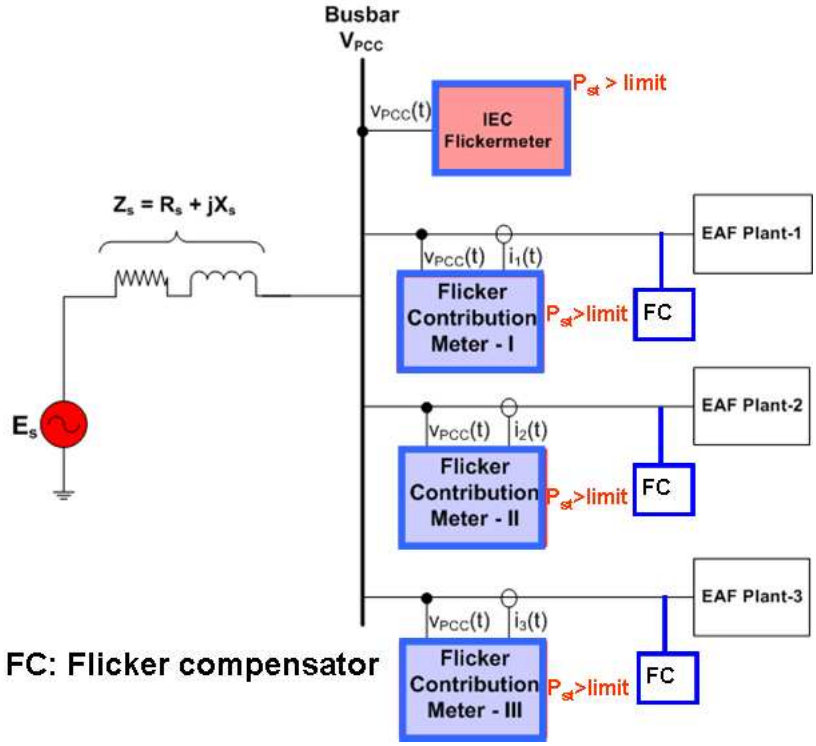

(a) Solution-1

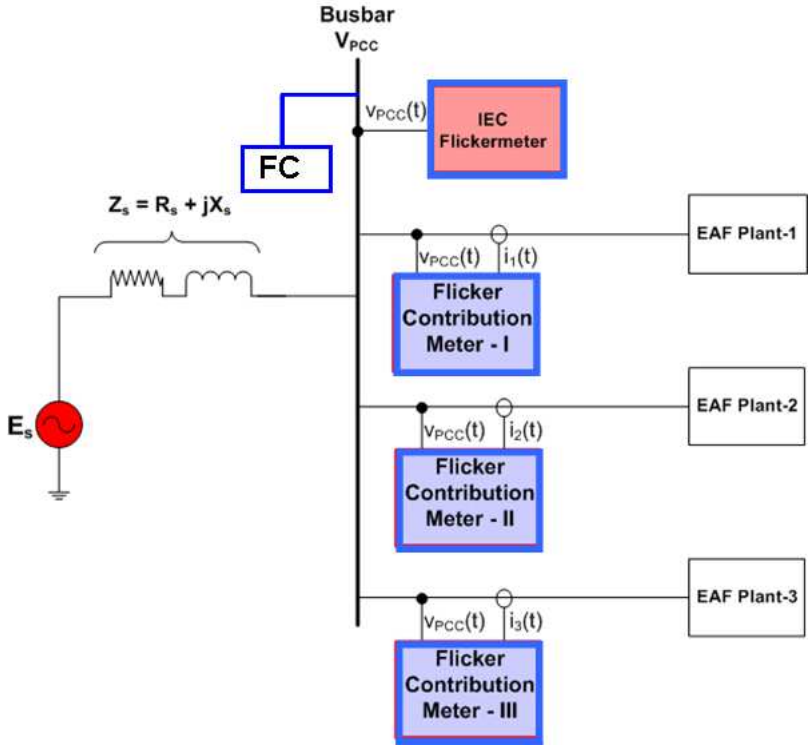

(b) Solution-2

Figure 4.2: Possible solutions to compensate flicker in Case 1.

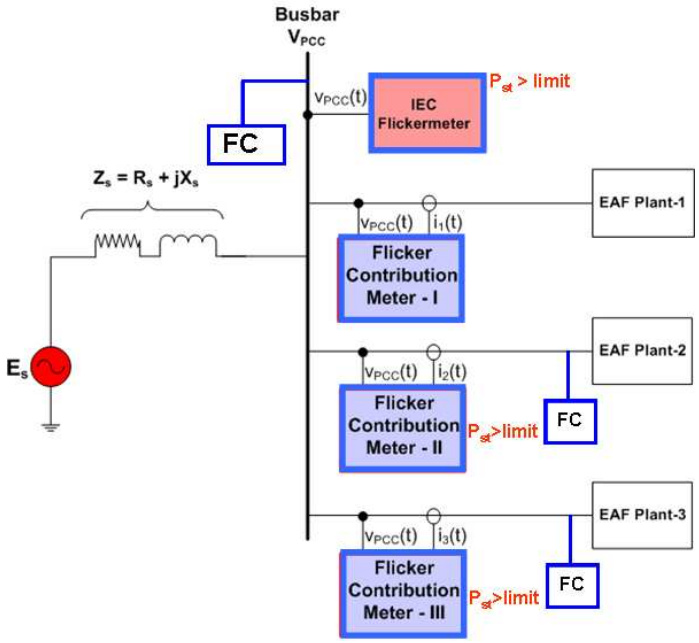

Figure 4.3: A possible solution to compensate flicker in Case 2.

Therefore, the utility should take necessary countermeasures in such a case. Solution can be connecting flicker compensator at the PCC or increase installed power of the utility in order to lower the system impedance or provide connection for one of the plants from another busbar. The ratio of the minimum short circuit power to the total apparent power of the arc furnaces at a busbar that gives energy to the arc furnace plants is recommended to be higher than 50 [19] [20] [21]. After the change of connection point for one plant, that bus should satisfy this ratio condition in order to solve the problem.

It is also worth to note that there may be situations when the flicker contributions of individual plants may exceed the limit but the total flicker at the busbar is below the limit, which is an unusual situation. Since the total flicker at that bus depends on the total load, (i.e the sum of all the currents) if the phases of the individual currents coincide such that the amplitude modulation on the total current is canceled out, the resultant flicker observed on the bus may be smaller than the individual contributions. This happens when the amplitude modulation of the currents are 180 degrees phase shifted with respect to each other. However the operation of electric arc furnaces are

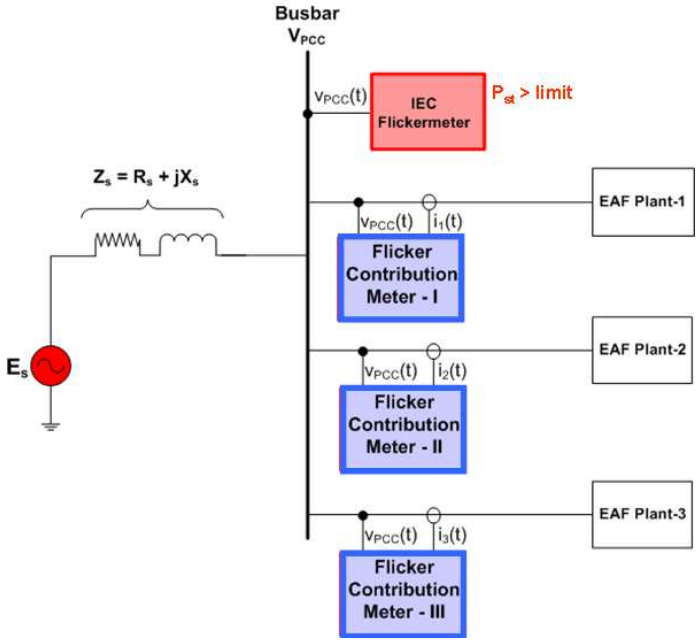

Figure 4.4: A possible solution to compensate flicker in Case-3.

very stochastic and this case rarely occurs.

CHAPTER 5

CONCLUSION

This thesis aims at investigating individual flicker contributions of multiple loads supplied from a point of common coupling (PCC). Flicker contribution of the specific load means, what the IEC flickermeter reading would be, if it were the only load supplied from the common bus with constant source voltage (i.e. no flicker effect coming from the supply side).

The results presented in the thesis show that source voltage is a time-varying quantity in an interconnected system, and the flicker measured at a PCC by the IEC flickermeter is not only caused by the consumer loads connected to that bus, but also by other flicker sources supplied from different PCCs in the neighborhood of the measured PCC. Therefore, a flicker contribution method is proposed in the thesis to decouple the flicker effects of the interconnected system (source side an upstream loads) and the loads, which utilizes reactive current component of each load and the source-side impedance seen from the PCC.

The proposed method uses voltage and current measurements of the individual loads together to reconstruct a fictitious PCC voltage from the Thevenin equivalent circuit of a grid supplying power to the intermittent loads. This fictitious voltage variation is used to evaluate the flicker contribution. A flicker-contribution-meter, which we call FC^M, utilizing this method has been developed to make flicker contribution measurements practicable in the field. PQ^+ Analyzers developed through the National Power Quality Project of Turkey [16], have been used to develop FC^Ms, which is obtained by a software update of the PQ^+ Analyzer.

The verification of the proposed method is achieved by using field tests and it has been verified to provide satisfactory results. Flicker contributions of four iron and steel plants such as plants including DC EAFs, AC EAFs, induction furnaces and the combination of continuous rolling shop and organized small industrial zone, are measured by the proposed FC^Ms and the results are presented.

The advantage of the proposed method is that, not only the dominant flicker source at a PCC is determined, but also the quantity of flicker contribution of each source is evaluated individually. In this method, since the upstream system impedance seen from the PCC is used in the evaluation of flicker contribution, it is essential to know the system impedance precisely for accurate flicker contribution computations. It has been shown that both the seasonal system impedance provided by the utility or online estimated value of it can be used to obtain satisfactory results for flicker contribution.

To develop the FC^M concept further, various possible usages of the developed device are provided in Chapter 4. The FC^M can be used in the regions of the grid where there are multiple loads with highly fluctuating current demands and high flicker emissions. It has been shown that, it can also be used as a guide to plan the installation of new plants with possible high flicker emissions. In addition, the FC^M can be used to plan, where the new flicker compensators should be installed on the grid.

REFERENCES

[1] IEC Standard 61000-4-30, ”Testing and Measurement Techniques-Power Quality Measurement Methods”.

[2] X.Y.Xavier, M. Kratz ”Power System Flicker Analysis by RMS Voltage Values and Numeric Flicker Meter Emulation”, IEEE Transactions on power delivery vol. 24, no. 3, July 2009

[3] IEC Standard 61000-3-3 ”Limits - Limitation of voltage changes, voltage fluctuations and flicker in public low-voltage supply systems, for equipment with rated current ¡ 16 A per phase and not subject to conditional connection”.

[4] R.C. Dugan, M.F.McGranaghan, S.Santoso, H.W.Beaty, ”Electrical Power Systems Quality ”, 2003 - New York McGraw-Hill.

[5] IEC Standard 61000-4-15, ”Flickermeter - Functional and Design Specifications” CEI.

[6] B.W.Kennedy, ”Power Quality Primer”, 2000 - New York McGraw-Hill McGraw-Hill.

[7] IEC Standard 61400-21, ”Measurements and Assesment of Power Quality Characteristics of Grid Connected Wind Turbines”.

[8] A.B.Nassif, E.E.Nino, W.Xu,: ”A V-I slope-based method for flicker source detection”, Power Symposium, 2005. Proceedings of the 37th Annual North American, 23-25 Oct. 2005, pp. 364-367.

[9] D.Zhang, W.Xu, A.Nassif, ”Flicker source identification by interharmonic power direction”, Electrical and Computer Engineering, 2005. Canadian Conference on, 1-4 May 2005, pp.549-552.

[10] P.G.V. Axelberg, M.H.J.Bollen, I.Y.H.Gu, ”Trace of Flicker Sources by Using the Quantity of Flicker Power”, Power Delivery, IEEE Transactions on, vol. 23, no. 1, Jan. 2008, pp.465-471.

[11] A. Hernandez, J.G. Mayordomo, R.Asensi, L.F.Beites, ”A method based on interharmonics for flicker propagation applied to arc furnaces” Power Delivery, IEEE Transactions on, vol. 20,no. 3, July 2005, pp. 2334-2342.

[12] S.Perera, D.Robinson, S.Elphick, D.Geddy, N.Browne, V.Smith, V. Gosbell, ”Synchronized flicker measurement for flicker transfer evaluation in power systems”, Power Delivery, IEEE Transactions on, vol. 21, no. 3, July 2006, pp. 1477-1482.

[13] Y.Y.Hong, L.H.Lee, ”Stochastic voltage-flicker power flow”, Power Delivery, vol. 15, no. 1, Jan. 2000, pp. 407-411

[14] A.M. DAN, ”Identification of Flicker Sources”, 8.International Conference on Harmonics and Quality of Power,Athens Greece 14-16 Oct. 1998,Vol.2 pp 1179-1181

[15] B.Hughes, ”Source identification for voltage sag and flicker”, Power Engineering Society Summer Meeting, 2000. IEEE Volume 2, 16-20 July 2000 Page(s):911 vol. 2.

[16] Güç Kalitesi Milli Projesi, http://www.guckalitesi.gen.tr Last visited 28.04.2010

[17] K.O.H. Pedersen, A.H. Nielsen, N.K.Poulsen, ”Short-Circuit Impedance Masurement”, IEEE Proc.-Gener. Transm. Distrib. Vol.150. No.2, 2003.

[18] Enerji Piyasası Düzenleme Kurumu, Elektrik Piyasası Şebeke Yönetmeliği.

[19] O. Salor, B. Gultekin, S. Buhan, et.al, ”Electrical Power Quality of Iron and Steel Industry in Turkey”, Industry Applications Conference, 42nd IAS Annual Meeting, pp. 404-423, 2007.

[20] B.Bharat, ”Arc Furnace Flicker Measurement and Control”,IEEE Trans.on Power Delivery, Vol.8, No.1, January 1993, pp.400-410.

[21] S.R.Mendis, M.T.Bishop, J.F.Witte, ” Investigations of Voltage Flicker in Electric Arc Furnace Power Systems”, IEEE Industry Applications Magazine, January/February 1996, pp.28-38.

[22] T.Demirci, A. Kalaycioglu, O. Salor, et.al. ”National PQ Monitoring Network for Turkish Electricity Transmission System”, IEEE Instrumentation and Measurement Technology Conference, Warsaw, Poland, May 1-3, 2007.

[23] E.Altintas, O.Salor, I.Cadirci, M.Ermis, ”A New Flicker Contribution Tracing Method Based on Individual Reactive Current Components of Multiple EAFs at PCC”, Industry Applications Conference, 44nd IAS Annual Meeting, 2009.

.

APPENDIX A

THE IEC FLICKERMETER

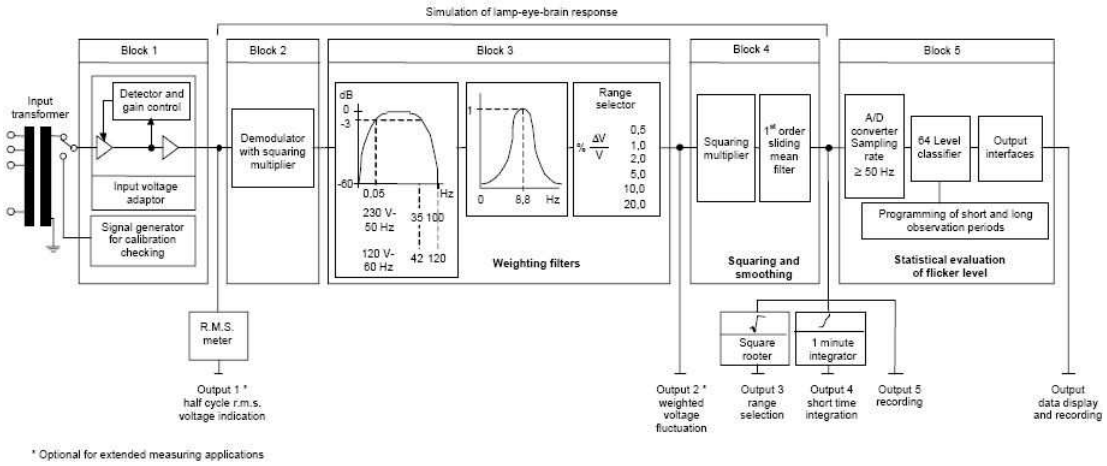

Figure A.1: Functional diagram of IEC flickermeter [5]

Functional diagram of the IEC flickermeter is given in Figure A.1. Block 1 is the input voltage adaptor. The output of the flickermeter must not be effected by the voltage level supplied to the device. Therefore a normalization block, which normalizes the input signal by its 10-min rms value, is used. The second block is a squaring block. It is used for demodulating the envelope of the normalized signal. The first filter on the third block eliminate DC offsets. It is a 1^{st} order high pass filter with 0.05 Hz cut off frequency. A 6^{th} order Butterworth low pass filter with cut off frequency of 35 Hz is used to filter out the components with frequency equal to twice the line frequency caused by the squaring operation. A weighting filter is used to weight the signal to simulate the lamp-eye response. It is a band pass filter with a gain of 1 at 8.8 Hz. Finally, in Block 4, the output of the 3^{rd} block is squared and a 1^{st} order sliding mean

filter with a time constant of 300 msec is used to resemble the brain response. The output of block 4 is the instantaneous flicker level.

Block 5 takes the output of block 4 (IFL, instantaneous flicker level) and performs a statistical analysis to provide a short term flicker level (P_{st}). By using P_{st}s, long term flicker level (P_{lt}) is calculated. P_{st} is evaluated in 10-min intervals and P_{lt} is evaluated in 2-hour intervals.

10-min short term flicker is evaluated with the formula given below which is given in the IEC standard.

$$P_{st} = \sqrt{0.0314P_{0.1} + 0.0525P_{1s} + 0.0657P_{3s} + 0.28P_{10s} + 0.08P_{50s}} \qquad \text{(A.1)}$$

Multipliers $P_{0.1}$, P_{1s}, P_{3s}, P_{10s}, P_{50s} given in the equation above are the levels of instantenous flicker severity that is exceeded in 0.1%, 1%, 3%, 10%, 50% time of the total 10 min observation time, respectively. Figure A.2 illustrates time interval where the IFL exceeds a certain level to make the P_x concept clear. These smoothed multipliers are obtained by the following equalities:

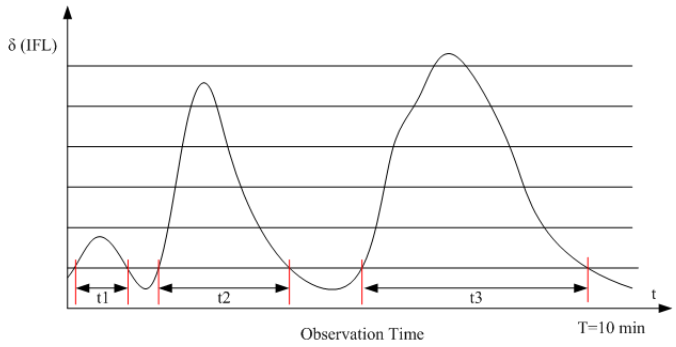

Figure A.2: Time variations of the instantaneous flicker (IFL) signal

$$P_{50s} = \frac{P_{30} + P_{50} + P_{80}}{3}$$
$$P_{10s} = \frac{P_6 + P_8 + P_{10} + P_{13} + P_{17}}{5}$$
$$P_{3s} = \frac{P_{2.2} + P_3 + P_4}{3}$$
$$P_{1s} = \frac{P_{0.7} + P_1 + P_{1.5}}{3}$$

Long term flicker severity is obtained from the short term values with the following formula:

$$P_{lt} = \sqrt[3]{\frac{\sum_{i=1}^{12} P_{sti}^3}{12}} \tag{A.2}$$

APPENDIX B

STANDARD LIMIT FOR FLICKER

Table B.1: The maximum flicker levels allowed by Electricity Market Grid Code [18]

Voltage Level (V)	**Flicker Severity**	
	Pst	**Plt**
$V > 154kV$	0.85	0.63
$34.5kV < V < 154kV$	0.97	0.72
$1kV < V < 34.5kV$	1.15	0.85
$V < 1kV$	1.15	0.85

In IEC Standart [5] Annex A.6.2.3, the evaluation techniques are recommended such that the flicker emission of a plant may exceed the given limits on 1% of the time observed for the short term flicker and 5% of the time observed for Plt.